Coordination Chemistry Reviews 253 (2009) 1495–1516

Contents lists available at ScienceDirect

Coordination Chemistry Reviews

journal homepage: www.elsevier.com/locate/ccr

Review

Platinum complexes of terpyridine: Interaction and reactivity with biomolecules

Scott D. Cummings*

Department of Chemistry, Kenyon College, Tomsich Hall, Gambier, OH 43022, United States

Contents

* Tel.: +1 740 427 5355.
E-mail address: cummingss@kenyon.edu.

doi:10.1016/j.ccr.2008.12.009

ARTICLE INFO

Article history:
Received 21 August 2008
Accepted 10 December 2008
Available online 24 December 2008

Keywords:
Platinum complexes
Terdentate nitrogen ligands
Intercalation
DNA
Protein labeling

ABSTRACT

Research on the coordination chemistry of Pt(II) terpyridine complexes spans more than 75 years, with significant recent work exploring the bioinorganic and medicinal chemistry of this diverse and versatile family of coordination compounds. This paper reviews the research literature describing investigations of the interactions of Pt(II) terpyridine complexes with nucleic acids and proteins.

1. Introduction

Research into the reactivity and interactions between transition metal complexes and biomolecules such as DNA and proteins has resulted in significant advances in the understanding of biochemical processes and the development of therapeutic drugs. Coordination compounds of platinum have an especially rich history due to the clinical success of cisplatin and related anti-cancer drugs. A large and growing family of Pt(II) complexes of 2,2′:6′,6″-terpyridine (terpy) have been receiving increased attention in bioinorganic and medicinal chemistry.

Forty years after the seminal paper in 1934 describing the syntheses of the first Pt(II) terpy complexes [1], Lippard and co-workers published the first report describing binding of Pt(II) terpy complex cations to DNA [2]. In recent years, Pt(II) terpy coordination compounds have become important reagents for the study of biomolecules due to their propensity to bind, often by selective modes, to nucleic acids [3] and proteins [4,5]. Investigations of biomolecular structure and reactivity are facilitated by the useful properties of Pt(II) terpy probes: the spin-active ^{195}Pt nucleus for NMR spectroscopy, the large Pt nucleus to serve as a high-scattering atom for X-ray diffraction studies, and long-wavelength light absorption and emission for identifying binding modes and changes in microenvironment of the probe [6].

In recent years, an explosion of interest in the platinum terpy family of complexes has resulted in as many as 30 new papers appearing annually in the primary literature. The purpose of this review is to present a comprehensive summary of the research of the interaction of platinum terpyridine complexes with biomolecules, work that has appeared in more than a hundred papers spanning three decades. A companion review focuses on the synthesis, reactivity and structural characterization of diverse members of the family of platinum (II) terpy complexes [7]. These complex cations can be represented by the formula $[Pt(Yterpy)X]^{n+}$, where X represents ligands occupying the fourth coordination site, Y represents substituents on the terpy ligand (in the 4′ position, unless otherwise noted) and n is the charge of the complex (Fig. 1). For example, $[Pt(Clterpy)Me]^+$ refers to methyl 4′-chloro-2,2′:6′,6″-terpyridine platinum (2+).

Much of the chemistry described in this review can be related to two intrinsic properties of $[Pt(Yterpy)X]^+$ complex cations [7]: (1) ease of displacement of the X ligand by nucleophiles and (2) the propensity for stacking of the terpy ligand with other π systems. However, members of the growing family of Pt(II) terpy complexes can be differentiated by a variations in charge, aqueous solubility, steric bulk, reactivity and redox and excited-state properties. At this stage in the development of the research field, rational design of Pt(II) complexes for specific biochemical applications can be accomplished through variation in the X ligand or modification of the terpy ligand, thereby tuning properties of the complex or interactions with specific biomolecules.

2. Interaction and reactivity with nucleic acids

Investigations of the binding of Pt(II) terpy complexes to DNA and RNA have revealed two primary modes of binding: intercalation between base pairs in the double helix and covalent bonding to individual bases or derivatized phosphates [3].

2.1. Intercalation

Intercalation is a common mode by which numerous drugs, antibiotics and dyes bind between base pairs of nucleic acid polymers, facilitated by non-covalent interactions between the π systems of the heterocyclic bases. Classic intercalators include ethidium bromide (an antimicrobial agent), proflavine and aminoacridine (dyes), doxorubicin (chemotherapeutic drug) and daunomycin and actinomycin D (antibiotics). DNA intercalation can be quantified by the following parameters:

K = binding equilibrium constant;
r_f = ratio of added intercalator concentration to total nucleotide concentration P_0;
r = ratio of bound intercalator concentration to total nucleotide concentration P_0 ($r = r_f$ for quantitative binding).

The first experimental evidence that Pt(II) terpy complex cations can bind to DNA appeared in a 1974 report by Lippard and co-workers [2], although previous work had suggested that $[Pt(terpy)Cl]^+$ may intercalate into *E. coli* tRNA [3]. The former study focused on the complex $[Pt(terpy)(HET)]^+$ (where HET = 2-hydroxyethanethiol, shown in Fig. 2) so as to avoid complications from chloride ligand displacement (see below). Evidence for intercalative binding came from observations that addition of

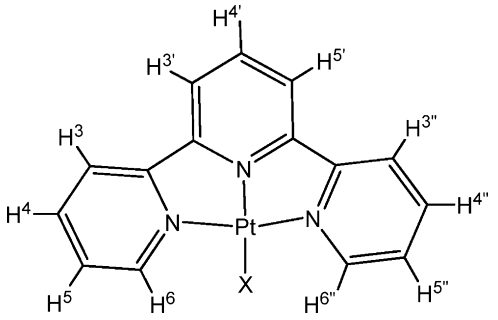

Fig. 1. $[Pt(terpy)X]^{n+}$ complex cation, showing atom numbering scheme.

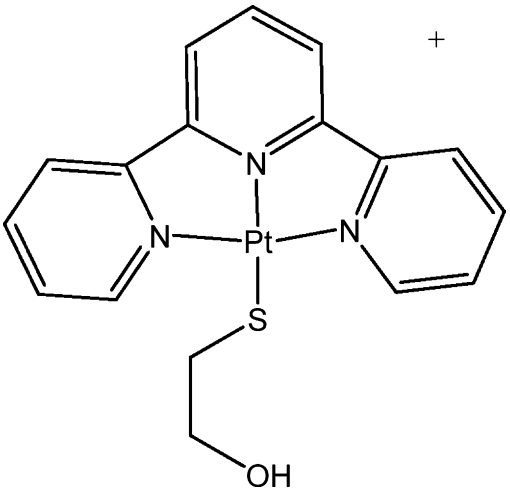

Fig. 2. Structure for [Pt(terpy)(HET)]$^+$.

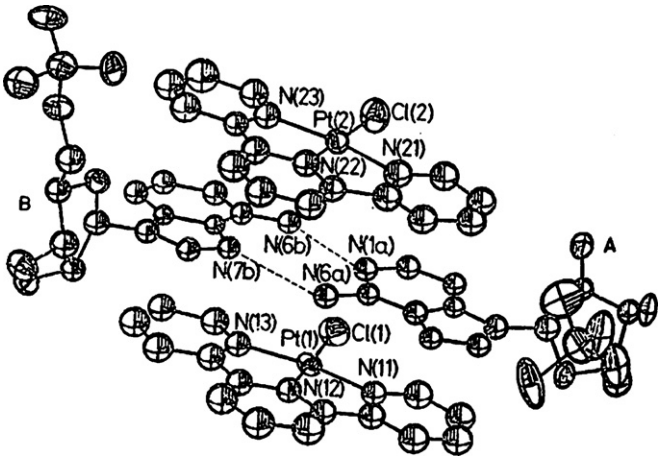

Fig. 4. Structure of the 2:2 intercalation complex formed between [Pt(terpy)Cl]$^+$ and AMP; from Ref. [12] (reproduced by permission of The Royal Society of Chemistry).

[Pt(terpy)(HET)]$^+$ to calf thymus DNA (ct-DNA) results in (1) competitive inhibition of ethidium fluorescence; (2) the induction of a circular dichroism (CD) spectrum; (3) an increase in the melting temperature, and therefore the stability, of the DNA duplex; (4) an increase in the viscosity of the DNA as a result of lengthening of the biopolymer. A binding constant of $K = (1.2 \pm 0.2) \times 10^6\ M^{-1}$ (for buffer solution having pH 6.8, 0.003 M NaCl) and a binding ratio of 0.20 platinum complex cations per nucleotide were calculated from spectrophotometric data. The binding is reversible upon dialysis of the DNA, but this complex does not covalently bind to, or nick, DNA. A report by Gabbay et al. added further support for intercalation into salmon testes (st) DNA, using results of circular dichroism, flow dichroism, ^{1}H and ^{13}C NMR spectroscopy experiments; they also note a second electrostatic binding at higher $r_f < 2$ [8]. McMillin and co-workers reported that when this complex cation binds to salmon testes (st) DNA the charge-transfer absorption band at 475 nm shifts to ca. 540 nm [9]. A recent report by Messori et al. compared intercalative binding of [Pt(terpy)Cl]$^+$ with proposed external DNA binding of [Au(terpy)Cl]$^{2+}$ [10].

2.1.1. Structure of the intercalation complex

X-ray diffraction photographs of hydrated crystalline fibers of calf thymus DNA containing intercalated [Pt(terpy)(HET)]$^+$ provided the first evidence supporting a binding model for which, at saturation, every other inter-base pair site is occupied by an intercalator (known as the nearest-neighbor exclusion effect) [11]. Diffraction data indicates a helix with Pt atoms repeating each 10.2 Å. A model of the intercalated Pt(II) terpy complex cation is shown in Fig. 3. Of note in the crystal structure is hydrogen-bonding between the hydroxyl group of the HET ligand and a phosphate ester of what would become the minor groove of an analogous DNA polymer.

The crystal structure for the 2:2 intercalation complex formed from the mixing of [Pt(terpy)Cl]$^+$ and adenosine-5′-monophosphate (AMP), shown in Fig. 4, displays a linear chain

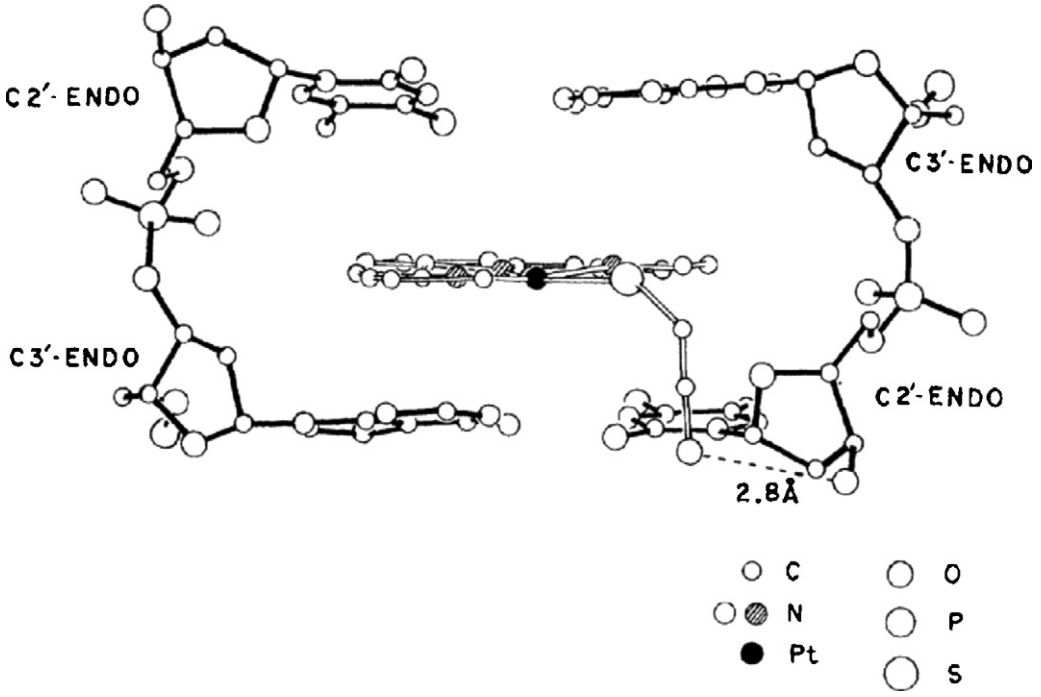

Fig. 3. Model of the intercalation complex formed between [Pt(terpy)(HET)]$^+$ and ct-DNA; from Ref. [11] (reproduced with permission of Stephen J. Lippard).

of tetrads comprised of a hydrogen-bonded base pair (with the uncommon Watson–Crick–Hoogsteen pairing) intercalated between two Pt(II) terpy units having head-to-head orientation [12]. The effect is essentially a reverse of the nearest-neighbor exclusion observed for platinum intercalation in DNA, present here even in the absence of the DNA polymer backbone and helix structure and indicating the importance of electrostatic and π-stacking forces to intercalation.

An interesting comparison of the latter structure is provided by the crystal structure for the neutral 2:2 intercalation complex formed from the mixing of $[Pt(terpy)(HET)]^+$ and deoxycytidylyl-(3′,5′)-deoxyguanosine (dCpG), shown in Fig. 5 [13]. One Pt(II) terpy cation intercalates in between two sets of hydrogen-bonded (typical Watson–Crick) G–C base pairs, with two additional Pt(II) terpy cations (having some disorder due to orientation of the HET ligands) capping each end. Several features suggest important structural factors for Pt(II) terpy intercalators: (1) significant overlap of the π systems of the terpy ligand and the bases, (2) orientation of O^6 atoms of the guanine bases directly above and below (and 3.4 Å away from) the Pt atom, and (3) orientation of the HET ligand side chain of the intercalated $[Pt(terpy)(HET)]^+$ into what would become the *major* groove of an analogous DNA polymer while those of the capping complex cations point toward the minor groove.

The trimetallic complex cation $[\{(terpy)Pt(SCH_2CH_2NH_2)\}_2Pt]^{4+}$ crystallized as an adduct with deoxymethoxy-pTpA, yielding a structure having A–T base pairs stacked on either side of stacked Pt(terpy) units [14]. A related diastereomer (Fig. 6), differing in relative orientation of the stacked Pt(terpy) units, was prepared but presumed to not intercalate due to an inability to nick closed DNA [15].

2.1.2. Effect of variation in platinum intercalator structure

While McFayden et al. note that free terpy is not capable of DNA intercalation at physiological pH [16], numerous Pt(II) complexes of terpy have been identified as metallointercalators. The binding affinity of Pt(II) terpy metallointercalators depends on several structural factors, including: (1) size and steric effects, (2) hydrogen-bonding capability, and (3) complex charge. Direct comparisons of binding equilibrium constants from different studies is complicated by the fact that *K* values are known to be very sensitive to solution ionic strength and DNA base composition (see below) as well as pH and temperature.

2.1.2.1. Mononuclear complexes. Lippard and co-workers investigated a larger family of Pt(II) and Pd(II) complexes for the effect of structure and charge of on DNA binding and nicking [17]. Included in the study were a group of five Pt(II) terpy complex cations of the type $[Pt(terpy)X]^{n+}$, for which $n = 1$ and X = Cl, HET, cysteine (Cys), or carboethoxymethanethiol (CMT); or $n = 2$ and X = 2-aminoethanethiol (AET). Each of these complex cations competitively inhibits ethidium binding to DNA and unwinds closed circular DNA, both effects indicative of intercalative binding. In addition, the CMT complex displays evidence of covalent binding. The AET complex possesses the highest binding constant (see Table 1), suggested to be due to the dicationic charge. For the HET complex, hydrogen bonding of the thiol tail may stabilize intercalation at other base pair sites and make this complex slightly less selective at lower [Pt]/[DNA] ratios [18]. Comparing a set of $[Pt(terpy)X]^{n+}$ complex cations to various Pt(II) bipyridine and phenanthroline complex cations suggests that a balance of structural factors affect binding constants [17,18]. In general, binding appears to be enhanced by (1) an increase in the positive charge of the complex cation, (2) a greater number of co-planar aromatic rings, and (3) the presence of an X ligand having hydrogen-bonding capability.

Results from other studies also indicate that the nature of the thiol ligand affects DNA binding. Relative to $[Pt(terpy)(HET)]^+$, the aliphatic thiol complex $[Pt(terpy)(SC_4H_9)]^+$, which lacks the hydrogen-bonding thiol tail, intercalates with a slightly lower binding constant [19,20], while the aromatic thiol complex $[Pt(terpy)(SPh)]^+$ intercalates into DNA even more weakly (see Table 1) [21]. For both of these complexes, an additional non-intercalative binding mode dominates at higher r_f.

The rate of binding of $[Pt(terpy)(SPh)]^+$ to ct-DNA was too rapid for observation using stopped-flow spectrophotometry, so estimated to exceed 10^7 M/s [21]. An investigation of the dissociation rates, using surfactant systems to sequester the platinum complex cation, revealed complex kinetics [21].

McMillin and co-workers reported that the hydroxo complex $[Pt(terpy)(OH)]^+$ binds to st-DNA initially via intercalation with a binding constant of $K \approx 7 \times 10^4\ M^{-1}$ [9]. Evidence for this binding mode comes from characteristic changes in the intensities of intraligand $\pi-\pi^*_{terpy}$ absorption bands and a bathochromic shift of the charge-transfer absorption band in the UV–vis spectrum, emergence of luminescence and circular dichroism, and a doubling of the DNA viscosity; covalent binding is a secondary binding mode for this complex (see below).

The dicationic pyridine complex $[Pt(terpy)(4\text{-picoline})]^{2+}$ binds very strongly to DNA via intercalation, as evidenced by gel electrophoresis of products and changes to UV–vis absorption spectrum and DNA melting temperature [22,23]. For $r_f < 0.16$, changes in the CD spectrum of poly[d(A–T)]$_2$ DNA were used to determine a binding constant of $K = (1.8 \pm 0.5) \times 10^7\ M^{-1}$ and a binding site size of every 4 base pairs, suggesting that the dicationic nature of this intercalator limits near-neighbor binding mode. However, weaker nearest neighbor binding mode emerges when $r_f > 0.18$.

An important study by Cusamano et al. showed how a balance of steric and electronic effects of pyridine ligands can affect the strength of intercalation into ct-DNA [23]. Trends in binding constants for the series of dicationic complexes having X = pyridine, 2-picoline and 4-picoline (Table 1) indicate that electron donation enhances intercalation by the 4-picoline complex and steric hindrance inhibits binding by the 2-picoline complex [23]. The related dicationic complex $[Pt(QT)]^{2+}$ (where QT = 2,2′:6′,2″:6″,2‴-quaterpyridine) binds to ct-DNA, but reported binding constants vary by an order of magnitude [23,24].

Scolaro and co-workers explored steric effects for a series of organometallic intercalators $[Pt(terpy)Me]^+$, $[Pt(Phterpy)Me]^+$, $[Pt(terpy)Ph]^+$, and $[Pt(Phterpy)Ph]^+$ [25]. Data from UV–vis and CD spectroscopy, electrophoresis and duplex melting studies indicated that only $[Pt(terpy)Me]^+$ intercalates into ct-DNA. In contrast, the binding constant for $[Pt(o\text{-tolyl-terpy})(2\text{-picoline})]^{2+}$ is reported to be the same as that for $[Pt(terpy)(2\text{-picoline})]^{2+}$, indicating that 4′ substituents on the terpy ligand do not affect intercalation [26]. Intercalation into ct-DNA is not prevented by the steric bulk of the carboranethiol ligand in complex cations such as $[Pt(terpy)(SCH_2C_2B_{10}H_{11})]^+$ [27].

Che and co-workers investigated DNA binding by a series of luminescent $[Pt(Yterpy)X]^+$ complexes using restriction endonuclease fragmentation assays, UV–vis absorption and luminescence spectroscopy, and gel electrophoresis [28]. Binding constants for intercalation of the terpy complexes having X = Cl, Ph, glycosylated acetylide or glycosylated arylacetylide (Table 1) are similar to those for other Pt(II) terpy complexes.

For a related complex having bulky *t*-butyl groups on the 4,4′ and 4″ positions of the terpy ligand, the DNA binding mode is proposed to be groove binding.

2.1.2.2. Polynuclear complexes. Several research groups have investigated DNA binding of dinuclear Pt(II) terpy complexes (commonly called "dimers") such as alkane dithiol-bridged dimers of the type

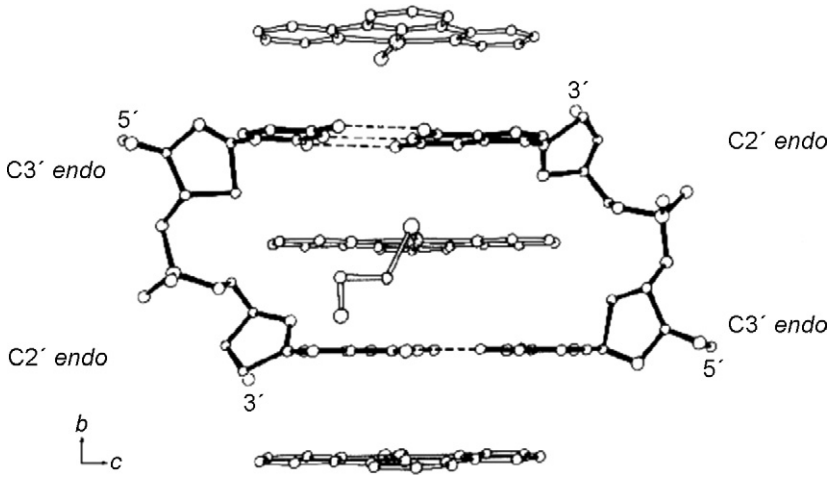

Fig. 5. Structure of the 2:2 intercalation complex formed between [Pt(terpy)(HET)]$^+$ and deoxycytidylyl-(3′,5′)-deoxyguanosine; from Ref. [13]. Reprinted by permission from Macmillan Publishers Ltd.: Nature, copyright 1978.

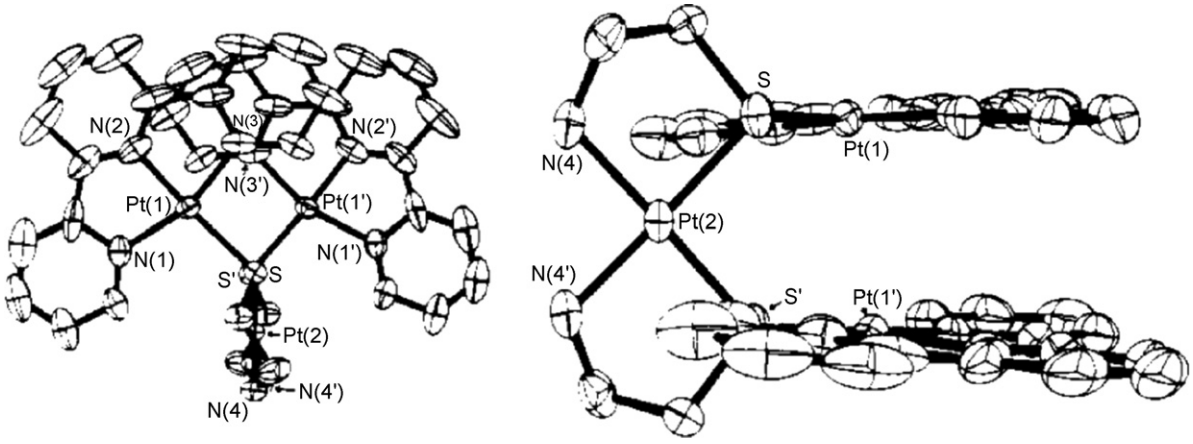

Fig. 6. A trinuclear complex cation containing two co-planar Pt(II) terpy units; from Ref. [15] (reproduced by permission of The American Chemical Society).

Table 1
Binding constants for Pt(II) terpy complex DNA intercalators.

Complex	DNA; medium	K (M^{-1})	Reference
[Pt(terpy)Cl]$^+$	ct-DNA; Tris buffer	3.9×10^5	[10]
[Pt(terpy)(HET)]$^+$	ct-DNA; pH 6.8, 0.003 M NaCl	1.2×10^6	[2]
[Pt(terpy)(HET)]$^+$	ct-DNA; pH 7.5, 0.2 M NaCl	1.2×10^5	[17]
[Pt(terpy)(AET)]$^{2+}$	ct-DNA; pH 7.5, 0.2 M NaCl	4.3×10^5	[17]
[Pt(terpy)Cys]$^+$	ct-DNA; pH 7.5, 0.2 M NaCl	1.0×10^5	[17]
[Pt(terpy)(CMT)]$^+$	ct-DNA; pH 7.5, 0.2 M NaCl	5×10^4	[17]
[Pt(terpy)(SPh)]$^+$	ct-DNA; pH 7.5, I = 0.01 M	3.5×10^5	[21]
[Pt(terpy)(SPh)]$^+$	ct-DNA; pH 7.5, I = 0.10 M	1.8×10^4	[21]
[Pt(terpy)(SPh)]$^+$	ct-DNA; pH 7.5, I = 0.30 M	3.0×10^3	[21]
[Pt(terpy)(SC_4H_9)]$^+$	ct-DNA; pH 7.0, I = 0.01 M	4.5×10^5	[20]
[Pt(terpy)(SC_4H_9)]$^+$	ct-DNA; pH 7.0, I = 0.10 M	4.3×10^4	[20]
[Pt(terpy)(SC_4H_9)]$^+$	ct-DNA; pH 7.0, I = 0.50 M	8.4×10^3	[20]
[Pt(terpy)(OH)]$^+$	st-DNA; pH 9 0.05 M EPPS buffer	7×10^4	[9]
[Pt(terpy)(4-picoline)]$^{2+}$	AT-DNA; 0.01 M NaCl	1.8×10^7	[22]
[Pt(terpy)(4-picoline)]$^{2+}$	ct-DNA; pH 7.0, 0.15 M $NaNO_3$	5.3×10^4	[23]
[Pt(terpy)(2-picoline)]$^{2+}$	ct-DNA; pH 7.0, 0.15 M $NaNO_3$	3.0×10^3	[23]
[Pt(terpy)py]$^{2+}$	ct-DNA; pH 7.0, 0.15 M $NaNO_3$	3.5×10^4	[23]
[Pt(terpy)(C≡CPh)]$^+$	ct-DNA; Tris buffer	6.9×10^5	[10]
[Pt(terpy)(C≡CPh-glycoside)]$^+$	ct-DNA; Tris buffer	3.7×10^5	[10]
[Pt(terpy)(C≡C-glycoside)]$^+$	ct-DNA; Tris buffer	4.8×10^5	[10]
[Pt(*o*-tolyl-terpy)(2-picoline)]$^{2+}$	ct-DNA; pH 7.0, 10^{-3} M phosphate buffer	3.3×10^3	[26]
[Pt(QT)]$^{2+}$	ct-DNA; pH 7.0, BPE buffer	2.3×10^4	[24]

$[(terpy)PtS(CH_2)_nSPt(terpy)]^{2+}$ (n = 4–10) [19], and similar systems having a carborane spacer in the alkane bridge [29]. Calculations of helix extension parameters and helix unwinding angles (see below) from viscosity data indicated that dimers having n = 5, 6, 7 acted as bis-intercalators with both Pt(terpy) units binding, whereas results for the n = 4, 8, 9 and 10 complexes suggested a mixture of bis-intercalation and mono-intercalation. The association constant for the n = 6 dimer is 23 times greater than that for the related monomer $[Pt(terpy)(SC_4H_9)]^+$ [20]. However, this enhancement is far less than the maximum theoretical value obtained by simply doubling the Gibbs energy value for binding of the monomer, indicating the importance in considering the role of distortions of the complex cation, nucleic acid or alkyl chain linker for bis-intercalation. Molecular modeling results suggested potential binding modes that include (1) bis-intercalation with a single base pair or two base pairs sandwiched between two Pt(II) terpy units, or (2) intercalation of one Pt(II) terpy unit with the second binding externally on the DNA surface [19]. Bis-intercalation by the n = 5 and 6 complexes would violate the neighbor exclusion principle established for mononuclear Pt(II) terpy complexes (see above).

Dimers having two Pt(terpy) units bridged by the more rigid 1,3- or 1,4-benzenedimethanethiol were prepared by Goto and co-workers [30]. Based on changes in UV–vis absorption and CD spectra upon the addition of ct-DNA, the authors suggest that the complex having the 1,3-benzenedimethanethiol bridging ligand acts as a bis-intercalator and distorts the DNA structure, whereas the complex with the linear 1,4-benzenedimethanethiol bridge intercalates only one of the two Pt(terpy) units with no accompanying distortion (Fig. 7).

A series of five $[\{Pt(N_3terpy)\}_2L]^{4+}$ complexes having bridging L ligands consisting of pyridine end caps with ethynyl, *para*-phenylene and/or $[Pt(pyridine)_2(NH_3)_2]^{2+}$ spacer groups of varying length were prepared by Lowe et al. [31]. Because the dimers possess rigid and extended bridging ligands, they are anticipated to serve as bis-intercalators capable of cross-linking two DNA duplexes. In addition, the bridging ligand can be cleaved by thiols or cyanide, while the azide group of the terpy ligand can act as a photoaffinity label.

A seven-coordinate luminescent Nd(III) complex serves as a bridge of two $[Pt(terpy)(SPh)]^+$ units in a trinuclear system prepared by Pikramenou and co-workers [32]. While the relative geometry of the two Pt(II) terpy units is not confirmed, flow linear dichroism studies and MM2 calculations suggest that the complex acts as a bis-intercalator with an especially large binding constant of $K \geq 10^8\ M^{-1}$.

A novel bimetallic complex consisting of two potential metallointercalators (Fig. 8) bridged by peptides was prepared by Sheldrick and co-workers [33,34]. Titration with ct-DNA resulted in UV–vis absorption changes consistent with intercalation only of the dppz ligand of Ir(I) complex but not the terpy ligand, suggesting that dppz is the thermodynamically preferred intercalator and that the oligopeptide bridge is not long enough to allow for concomitant intercalation by the $Pt(terpy)^{2+}$ unit. The work also indicates that short peptide bridge may enhance surface π–π interactions between $[Pt(terpy)]^{2+}$ and DNA bases.

In addition to structural factors related to the nature of the metallointercalator, binding affinities also depends on other factors, including base pair composition of the nucleic acid and ionic strength of the medium.

2.1.3. *Effect of nucleic acid composition*

Pt(II) terpy complexes typically display selectivity toward nucleic acids rich in G·C base pairs. For example, the binding affinity of the metallointercalator $[Pt(terpy)(HET)]^+$ increases linearly with the G·C molar ratio present in various types of DNA [18]. The complex cations $[Pt(terpy)(SPh)]^+$ [21] and $[Pt(terpy)(OH)]^+$ [9] also display G·C base pair selectivity. The complex cation $[Pt(terpy)(SC_4H_9)]^+$ binds to poly(dG–dC)·poly(dG–dC) with a 12-fold enhanced association constant than for binding to poly(dA–dT)·poly(dA–dT) [20]. Pt(II) terpy dimers also display G·C base pair selectivity, but without enhancement over monomers [20]. In general, more polarizable intercalators have higher specificity for the more polarizable G·C base pair, but $[Pt(terpy)(HET)]^+$ also intercalates into nucleic acid polymers containing no G·C base pairs (see below) [35]. Two explanations of this selectivity have been proposed in the literature: a specific interaction between the

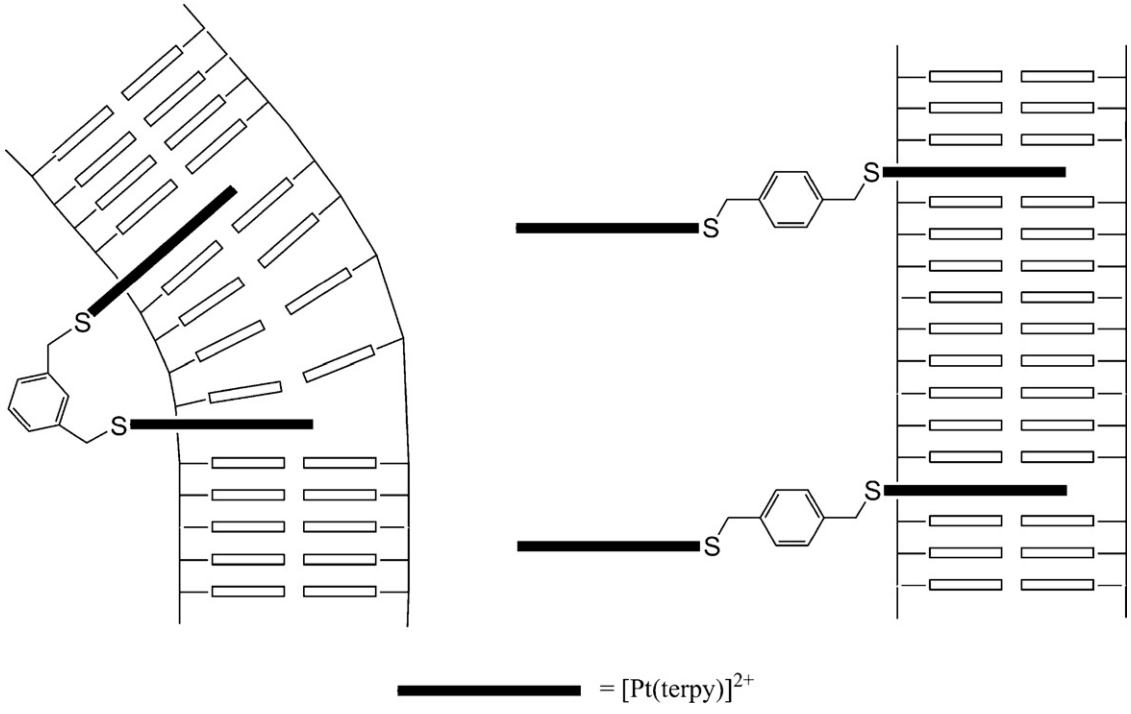

Fig. 7. Proposed mono- and bis-intercalation binding modes for the dinuclear complexes $[\{Pt(terpy)\}_2(benzenedimethanethiol)]^{2+}$ adapted from Ref. [30].

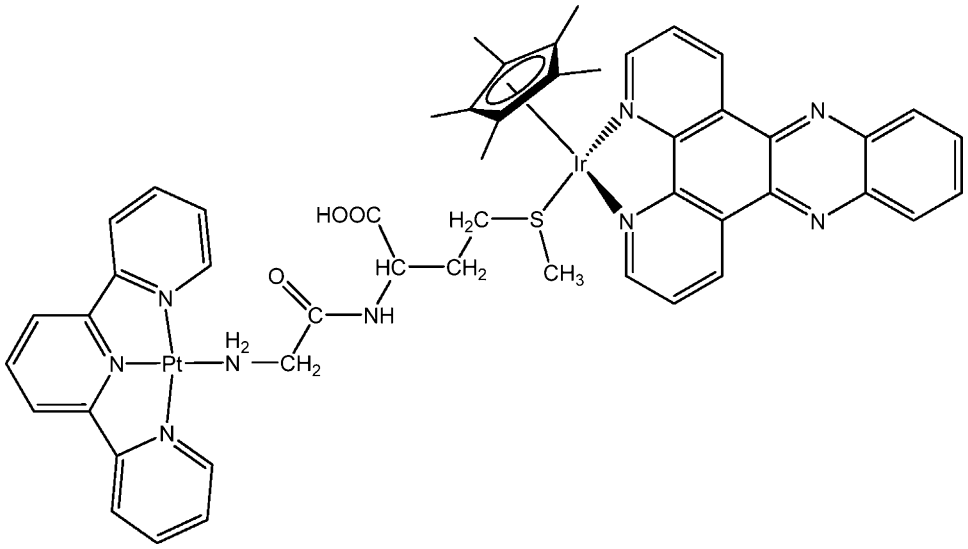

Fig. 8. A bimetallic DNA intercalator.

Pt^{2+} center and the residual negative charge on the O-6 atom of guanine, and π-orbital mixing between the electron-rich G·C base pair and the terpy ligand [21].

In contrast, the dicationic complex $[Pt(terpy)(4\text{-picoline})]^{2+}$ intercalates into poly[d(A–T)]$_2$ DNA with a binding constant that is orders of magnitude higher than that observed when using ct-DNA (Table 1) [23].

Pelleting experiments involving ultracentrifugation to separate bound and unbound intercalator complex showed that $[Pt(terpy)(HET)]^+$ binding to poly(A)·poly(U) and to poly(I)·poly(C) (I = inosine) RNA – but not to ct-DNA – is highly cooperative, with the binding of one platinum complex cation enhancing the binding of a second in a neighboring site [35]. At saturation, two platinum complex cations are bound in a three base pair site. These differences in binding to DNA and RNA suggest an ability of Pt(II) terpy complex cations to recognize differences in nucleic acid structures.

2.1.4. Effect of ionic strength and the thermodynamics of intercalation

The binding affinities of complex cations $[Pt(terpy)(HET)]^+$ [18] and $[Pt(terpy)(SC_4H_9)]^+$ to ct-DNA [20] are reduced under conditions of high solution ionic strength (e.g. $[Na^+] = 0.200$ M), for which electrostatic effects are minimized.

Investigations of the effect of ionic strength on binding affinity have been used to calculate association constants ($K_0^{1\ M}$) and Gibbs energy changes (ΔG) for intercalation in the absence of ionic charge effects. For $[Pt(terpy)(HET)]^+$, extrapolation of binding constant data to 1 M salt concentrations yields $K_0^{1\ M} = 3.7 \times 10^3\ M^{-1}$ [18]. Similar results were found for the complex cations $[Pt(terpy)(SC_4H_9)]^+$ ($K_0^{1\ M} = 4.1 \times 10^3\ M^{-1}$) [20] and $[Pt(terpy)(SPh)]^+$ ($K_0^{1\ M} = 1.7 \times 10^3\ M^{-1}$) [21]. Intercalation of the latter is driven by a favorable entropy change, and temperature-dependent investigations revealed that increasing salt (KF) concentration results in slightly more negative ΔH of binding but much less positive ΔS of binding [21].

2.1.5. Effect of intercalation on DNA structure

Intercalation typically results in a set of measurable changes in physical properties of DNA, including: an increase in DNA viscosity (due to lengthening and unwinding of the helix), release of cations (due to binding of cationic intercalator) and increase in the melting temperature (due to duplex stabilization in the region of the bound intercalator).

2.1.5.1. Helix extension and unwinding. Intercalation of Pt(II) terpy complex cations results in extension of the DNA helix (Fig. 9), although the effect generally is less than that observed when using classic organic intercalators such as proflavin and ethidium. While the earliest investigation of DNA binding by $[Pt(terpy)(HET)]^+$ provided evidence that intercalation results in an unwinding of the DNA helix [2], subsequent X-ray diffraction data were used to compute an unwinding angle of $22 \pm 6°$ [11]. In a study using polarized dynamic light-scattering measurements, Newman reported that addition of $[Pt(terpy)(HET)]^+$ to superhelical plasmid DNA first relaxes the helix then (for binding ratios beyond $r = 0.11$) over-winds the helix [36]. An NMR spectroscopic investigation showed that intercalation of $[Pt(terpy)(HET)]^+$ into DNA is accompanied by a large downfield shift in the phosphate ^{31}P signal, with a magnitude consistent with an unwinding angle of 18° [37]. Small-angle X-ray scattering studies of covalently closed circular DNA having intercalated $[Pt(terpy)(HET)]^+$ provided insight into the conformation of the plasmid and how the platinum intercalator unwinds and introduces kinks into the supercoiled structure [38]. Intercalation of $[Pt(terpy)(SC_4H_9)]^+$ into supercoiled DNA results in a helix unwinding angle of 17.5°, while related dimers $[(terpy)PtS(CH_2)_nSPt(terpy)]^{2+}$ ($n = 4$–10) lead to unwinding

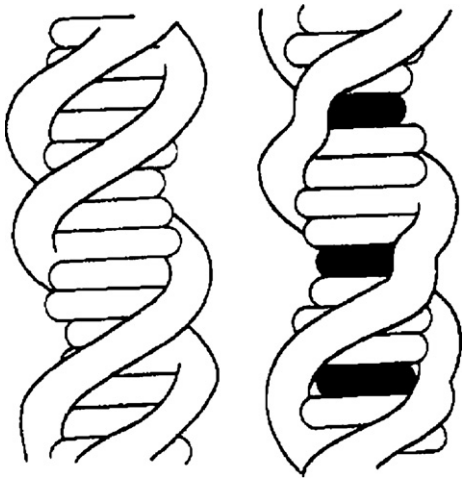

Fig. 9. The unwinding and lengthening of DNA that accompanies intercalation; from Ref. [3] (reproduced by permission of The American Chemical Society).

angles ranging from 22.9° to 36°, with the higher values consistent with a bis-intercalation mode [19]. Lowe and co-workers used a gel electrophoresis assay to show that unwinding of ct-DNA by $[Pt(terpy)(4\text{-picoline})]^{2+}$ intercalation yields topoisomeric circles [22].

For the metallointercalators $[Pt(terpy)(SPh)]^+$ and $[Pt(terpy)(SC_4H_9)]^+$, an increase of 2 Å in ct-DNA helix length was found for $r \leq 0.2$, as calculated from viscosity change measurements [19,21]. Fiber X-ray diffraction measurements of ct-DNA indicated that application of a powder of [Pt(terpy)Cl]Cl to the nucleic acid polymer results in lengthening of the helix by 10% [39].

While many studies of helix extension rely on the use of viscometers to measure changes in solution viscosity, a report by Yang and co-workers describes the use of a quartz crystal resonator as a more accurate and sensitive technique for investigating the effect of intercalation by the dicationic quaterpyridine complex $[Pt(QT)]^{2+}$ [24].

2.1.5.2. Cation release. Intercalation of $[Pt(terpy)(HET)]^+$ into ct-DNA results in the release of 1.5 cation equivalents, whereas ethidium and other platinum complex cations release only one cation equivalent. This excess cation release was initially attributed to result from hydrogen bonding of the HET tail to an adjacent phosphate group [18]. Results using $[Pt(terpy)(SC_4H_9)]^+$, for which only a slight excess (1.1 equivalents of K^+) is released, may support this hypothesis [20]. However, the complex cations $[Pt(terpy)(SPh)]^+$ also releases excess (1.4 equivalents) of cation upon intercalation [21]. An alternate hypothesis suggests that the Pt(II) terpy complex may have unusual effects on local charge density [21].

2.1.5.3. Duplex stabilization. Changes in several physical properties of poly(A)·poly(U) RNA upon intercalation of $[Pt(terpy)(HET)]^+$ were studied by Barton and Lippard [35]. The melting temperature (T_m) of the duplex polymer increases from 37 to 43 °C upon platination, indicating stabilization of helical over random coil RNA. Triple strand formation was ruled out.

Intercalation of $[Pt(terpy)Cl]^+$ into ct-DNA results in an increase in T_m by 3–5 °C [10,22], while the effect is larger for the methyl complex $[Pt(terpy)Me]^+$ ($\Delta T_m = 7.8$ °C) [40] and smaller for $[Pt(terpy)(SPh)]^+$ ($\Delta T_m = 3$ °C) [30]. The mono-intercalating dimer $[\{Pt(terpy)\}_2\{(1,4\text{-}SCH_2)_2C_6H_4\}]^{2+}$ increases T_m from 72 °C to 78.0 °C while the bis-intercalator $[\{Pt(terpy)\}_2\{(1,3\text{-}SCH_2)_2\text{-}C_6H_4\}]^{2+}$ dimer increases T_m to 82.5 °C [30]. Intercalation of $[Pt(terpy)(4\text{-picoline})]^{2+}$ results in two transitions, at $T_m = 75$ °C and 88 °C, attributed to separate melting at lower T for regions lacking intercalator and at higher T for regions stabilized by the platinum intercalator [22], but a subsequent study assigned the second transition to chemical reaction of the Pt(II) terpy complex [23].

2.2. Other modes of non-covalent binding to nucleic acids

While intercalation is the dominant non-covalent binding to double stranded DNA at lower r_f, weaker non-intercalative binding has been proposed for the complex cations $[Pt(terpy)(HET)]^+$, $[Pt(terpy)(SPh)]^+$ and $[Pt(terpy)(SC_4H_9)]^+$ at higher r_f [8,19–21]. Aggregates of $[Pt(terpy)(HET)]^+$ are also thought to play a role in cooperative binding to RNA [35]. At higher r_f, the organometallic complex cation $[Pt(terpy)Me]^+$ forms aggregates that bind to the surface of DNA [40,41].

The binuclear complex cation $[\{Pt(terpy)\}_2(Can)]^{3+}$ (where Can = canavanine), which *cannot* intercalate between base pairs due to a 6.0 Å thickness of the two stacked Pt(II) terpy units, does bind to DNA and a wide range of double-stranded and single-stranded oligonucleotides and polynucleotides via electrostatic and hydrophobic forces [42].

Investigations of the interaction of transition metal complexes with single stranded nucleic acids are far fewer than studies involving double stranded DNA. Wakelin et al. reported that the metallointercalator $[Pt(terpy)(SPh)]^+$ binds to single-strand DNA [21]. Calculations of a high binding affinity for the complex cation to thermally or chemically denatured DNA suggest a binding mode other than intercalation. The authors did not address whether this mode is a non-covalent π-stacking interaction or covalent binding via displacement of thiophenol.

Interaction of $[Pt(terpy)Me]^+$ with single-strand poly(5′-adenilic acid) and random coil poly(vinylsulfonate) results in disordered aggregate formation, as indicated by resonance light scattering and circular dichroism experiments [25]; this is in contrast to the highly organized assembly $[Pt(terpy)Me]^+$ forms with poly(L-glutamic acid) [43] (see Section 4).

A more recent paper reports the use of $[Pt(terpy)py]^{2+}$ to induce aggregation of poly-adenylic acid (PolyA), which serves as a model for single strand RNA [44]. At molar ratios of Pt/PolyA exceeding 0.4, aggregation occurs that was described as crosslinking of two PolyA strands by the Pt(II) terpy complex. While the authors did not postulate a specific structure, they noted the important role of the aromatic terpy ligand and the relatively minor role of charge balance by the cationic complex.

An important study by Yam and co-workers investigated the ability of single stranded olionucleotides to bind acetylide complexes $[Pt(terpy)(C{\equiv}C{-}C{\equiv}CH)]^+$ and the more water-soluble $[Pt(terpy)(C{\equiv}C{-}C{\equiv}COH)]^+$ [45]. Binding, which is thought to involve electrostatic attraction to the anionic phosphate groups, results in formation of platinum complex aggregates, as evidenced by long-wavelength absorption and luminescence bands; the effect is most pronounced for poly$(dA)_{25}$.

G-quadruplex DNA is also a target of binding by transition metal terpyridine complexes. Using two different biophysical assays (displacement of fluorescent thiozole orange and DNA melting), Teulade-Fichon and co-workers have shown that three Pt(II) terpy complexes bind to G-quadruplex DNA [46]. Enhanced binding for these square-planar complexes and related square-pyramidal Cu(II) terpy complexes over that for tetrahedral Zn(II) and octahedral Ru(II) terpy complexes indicates the importance of π–π interactions of the metal complex with external G-quartets of the DNA structure.

2.3. Covalent binding to nucleobases

In addition to non-covalent binding to nucleic acid polymers, $[Pt(Yterpy)X]^{n+}$ complex cations having a labile X ligand can undergo facile ligand substitution reactions to bind covalently to donor atoms of nucleobases. Ligand substitution reactions of the type (where Z is an incoming nucleophilic ligand):

$$[Pt(Yterpy)X]^{n+} + Z \rightarrow [Pt(Yterpy)Z]^{n+} + X$$

involve a combination of thermodynamic factors (relative stability of the Pt–X vs. Pt–Z bonds) and kinetic factors (rate of X ligand displacement by Z) [7]. Some reactions reach equilibrium while others are shifted to completion using an excess concentration of entering ligand. Complexes having $X = Cl^-$, H_2O, OH^- and pyridine derivatives are known to react with nucleobases.

2.3.1. Covalent binding to individual nucleobases

Early reports of covalent binding of $[Pt(terpy)]^{2+}$ to nucleobases (and related derivatives) relied on UV–vis spectroscopic data but provided no evidence of binding mode. For example, a slow reaction between $[Pt(terpy)Cl]^+$ and a mixture of adenosine-5′-monophosphate (AMP) and uridine-5′-monophosphate (UMP) was evident by changes in the UV–vis absorption spectrum of the

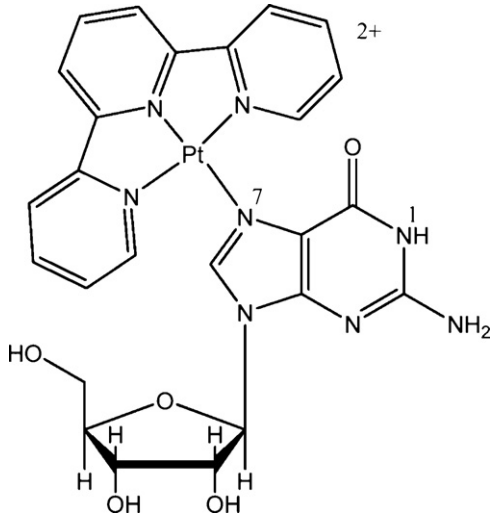

Fig. 10. Structure of the 1:1 complex of $Pt(terpy)^{2+}$ and guanosine.

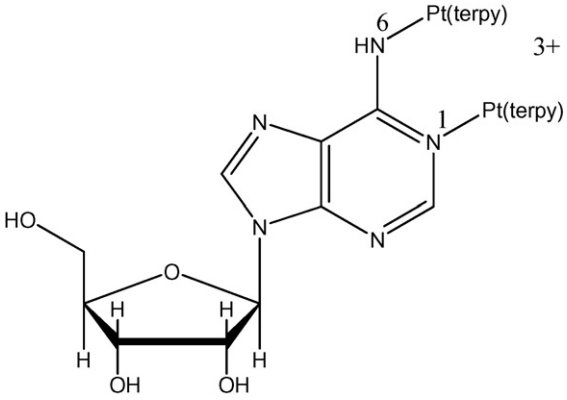

Fig. 11. Structure of the 2:1 complex of $Pt(terpy)^{2+}$ and adenosine.

complex, and Job's plots indicated two platinum binding sites for AMP, presumed by the authors to be the N^7 and N^1 positions [47]. Similarly, interaction between $[Pt(terpy)Cl]^+$ and ATP was proposed by Milanick on the basis of changes in the UV–vis spectrum of the mixture [48].

The first characterization of Pt(II) terpy nucleobase complexes came from detailed NMR spectroscopy investigations by Lowe and co-workers on the reactions of $[Pt(terpy)Cl]^+$ and $[Pt(terpy)(4\text{-picoline})]^{2+}$ with nucleosides guanosine (G), 2′-deoxyguanosine (dG), adenosine (A), 2′-deoxyadenosine (dA), 2′-deoxycytidine (dC) or thymidine (T) [49]. The complexes $[Pt(terpy)(G)]^{2+}$ or $[Pt(terpy)(dG)]^{2+}$ form quantitatively from the reaction of guanosine (G) or 2′-deoxyguanosine (dG) with $[Pt(terpy)Cl]^+$ in the presence of Ag(I) at pH 5.5–6 [49]. In contrast, incubation of $[Pt(terpy)(4\text{-picoline})]^{2+}$ with equimolar amounts of a G or dG at 37 °C for several days results in a slow reaction to displace 4-picoline, but produces an equilibrium mixture of the same product along with starting material. ^{1}H NMR spectroscopy and mass spectrometry results are consistent with a 1:1 Pt:G complex, with platinum binding to the N^7 atom of G or dG, as is common for many other Pt(II) reagents. Subsequent mass spectrometry investigations supported this assigned coordination mode (Fig. 10) [50]. Importantly, this binding site is not involved in Watson–Crick base pairing in helical DNA, suggesting that this position may be an available covalent binding mode in DNA.

Related work from van Eldik and co-workers showed that the aqua complex $[Pt(terpy)(OH_2)]^{2+}$ can bind rapidly at pH 2.5 to G, guanosine-5′-monophosphate (GMP), inosine (I) and inosine-5′-monophosphate (IMP) [51]. In each case, coordination is via the N^1 position because the N^7 position is protonated at this low pH. Extension of this research investigated the kinetics for the reaction between $[Pt(terpy)Cl]^+$ and GMP [52]. The guanosine ligand can be displaced at pH 6 by sulfur donor ligands cysteine, glutathione, thiourea, thiosulfate, and diethyldithiocarbamate [51]. Although formation of an adduct between $[Pt(terpy)Cl]^+$ and inosine-5′-monophosphate was reported, structural characterization was not given [9,52].

Reactions of Pt(II) terpy reagents with one equivalent of A (or dA) result in a tricationic product having two Pt(II) terpy units, one coordinated at the N^1 atom and a second at the exocyclic N^6 (deprotonated) amino group (Fig. 11) [49]. A similar product form using dC, with platination occurring at the N^3 and deprotonated amino N^4 positions (Fig. 12) [49]. The driving force to form dinuclear complexes may be attributed to the propensity for stacking of the two $Pt(terpy)^{2+}$ units in each of these products, an effect that is similar to stacking observed in solution, solid-state packing and the formation of other bridged dinuclear products [7]. Also, platination of the nitrogen atom on the ring may lead to increased acidity of the exocyclic amino protons.

Similarly, the reaction of 1-methylcytosine (Hmcyt) with one equivalent of $[Pt(terpy)Cl]^+$ in the presence of Ag(I) results in formation of $[Pt(terpy)(Hmcyt)]^{2+}$ while using two equivalents of platinum reagent results in the formation of the dimer $[\{Pt(terpy)\}_2(mcyt)]^{3+}$ [53]. A crystal structure of the monomer reveals binding through the N^3 position of the nucleobase, and ^{1}H NMR data indicate that this results in a pronounced increase in the acidity of the adjacent amino (N^4) group. Accordingly, binding occurs to the N^3 and deprotonated N^4 position in the dimer, resulting in stacked Pt(II) terpy units.

Reaction of either $[Pt(terpy)Cl]^+$ or $[Pt(terpy)(4\text{-picoline})]^{2+}$ with thymine results in slow reactions with mixtures of unidentified products [49].

Using electrospray ionization tandem mass spectrometry, Wee et al. identified gas-phase Pt(II) terpy complexes of nucleic acids (G, dG, dGMP, C, dC, dCMP, A, dA, dAMP) formed upon 24 h incubation of [Pt(terpy)Cl]Cl with each nucleobase in water; no thymine products formed using T, dT or dTMP [54]. In addition, the observation of peaks for oligomers $[Pt(terpy)(dG)_n]^{2+}$ ($n = 1$–13) ion fragments were attributed to ribbon structures of hydrogen-bonded deoxyguanines with a $[Pt(terpy)]^{2+}$ terminus. Collision-induced dissociation investigations revealed that the nucleic acid complexes displayed many fragmentation pathways but none involving the formation of nucleic acid radical cations.

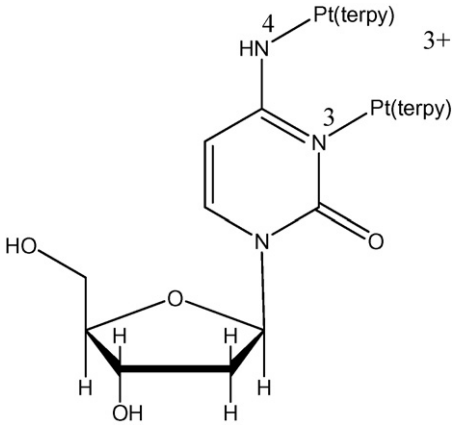

Fig. 12. Structure of the 2:1 complex of $Pt(terpy)^{2+}$ and 2′-deoxycytidine.

2.3.2. Covalent binding to bases in polynucleotides

Despite the research during the past decade to identify the specific platination sites for individual nucleobases G, C and A, characterization of binding modes of $[Pt(terpy)]^{2+}$ to polynucleotides is less advanced. The Lippard group's early studies of the reversible intercalation of $[Pt(terpy)Cl]^{+}$ into DNA also noted irreversible covalent binding modes but they did not identify specific coordination sites [2,17]. Recent work indicates that incubation of $[Pt(terpy)Cl]^{+}$ with ct-DNA for 24 h at room temperature results in approximately 30% covalently attached $Pt(terpy)_2{}^{2+}$, while the remaining platinum reagent can be removed using cation-exchange chromatography [55]. Lowe and co-workers found evidence of the dicationic complex $[Pt(terpy)(4\text{-picoline})]^{2+}$ binding covalently to ct-DNA, presumably due to displacement of 4-picoline by nucleobases [22]. Luminescence spectroscopy shows that the hydroxo complex cation $[Pt(terpy)(OH)]^{+}$ initially binds to DNA via intercalation but slowly displaces the hydroxo ligand and covalently coordinates to DNA, especially at lower r_f [9]. Reaction of the chloro complex with *E. coli* tRNA results in platinum binding to the lone sulfur donor atom in the polynucleotide (the thiocarbonyl group of a 4-thiouridine residue) and disruption of the tertiary structure of the biopolymer [3]. In contrast, addition of $[Pt(terpy)Cl]^{+}$ to poly(A–U) synthetic polynucleotide in 50 mM Tris buffer at pH 7.5 and 0.1 M NaCl results in essentially no binding [47].

Electron spray mass spectrometry experiments indicated that the reaction between the dinuclear complex $[\{Pt(terpy)\}_2$-*N*,*N*-4,4′-vinylenedipyridine$]^{4+}$ and the self-complimentary oligonucleotide d(CpGpTpApCpG) results in displacement of the dipyridyl bridge and the formation of trianionic adduct $[Pt(terpy)d(CpGpTpApCpG)]^{3-}$ [50]. Following enzymatic hydrolysis of this adduct, mass spectrometry of the platinum-containing product indicated the formation of $[Pt(terpy)(guanine)]^{2+}$ via loss of deoxyribose. Collision-induced dissociation mass spectrometry on the adduct indicated platination of the 3′ terminus of the oligonucleotide, and experiments using longer oligonucleotides indicate a selectivity for guanine binding [50].

Ford et al. reported an interesting reaction of platinated DNA [55]. Sodium borohydride or dimethylamine borane are capable of reducing covalently bound $Pt(terpy)^{2+}$ to form colloidal Pt(0) along the helix. Transmission electron microscopy was used to detect 1 nm size Pt particles. Subsequent treatment with a gold plating solution results in 1–7 nm particles formed from the platinum nucleation sites. This work informs efforts in an active research field working to build metallated DNA nanowires.

2.4. Binding to phosphate and phosphorothioate groups

With the goal of developing a heavy metal reagent to label specific bases in DNA or RNA for electron microscopy applications, Strothkamp and Lippard presented an approach relying on the propensity of $[Pt(terpy)Cl]^{+}$ to react with sulfur donor atoms[47]. Incorporated phosphorothioate groups into specific sites of a DNA or RNA polymer backbone allows for labeling by thiophilic metal reagent such as a Pt(II) terpy complex. The addition of one equivalent of the nucleosides uridine monophosphorothioate (UMPS) or adenosine monophosphorothioate (AMPS) to a solution of $[Pt(terpy)Cl]^{+}$ results in a rapid color change. The absorption spectra of the resulting solutions are very similar to that of the thiolate complex $[Pt(terpy)(HET)]^{+}$, suggesting a S-bound nucleoside complex (Fig. 13), but excess platinum reagent also leads to base binding. UMPS can displace coordinated AMP or UMP, also.

UV–vis absorption and radiolabeling experiments indicated that binding of $[Pt(terpy)Cl]^{+}$ occurs readily to the phosphorothioate-derivatized copolymer poly($_S$A-U), which consists of alternating AMPS and UMP [47]. Binding is quantitative up to $r_f = 0.50$, but not complete until $r_f = 2$. No binding to poly(A–U) is observed under similar conditions, again indicative of S atom binding of the Pt(II) cation. Lippard and co-workers also investigated

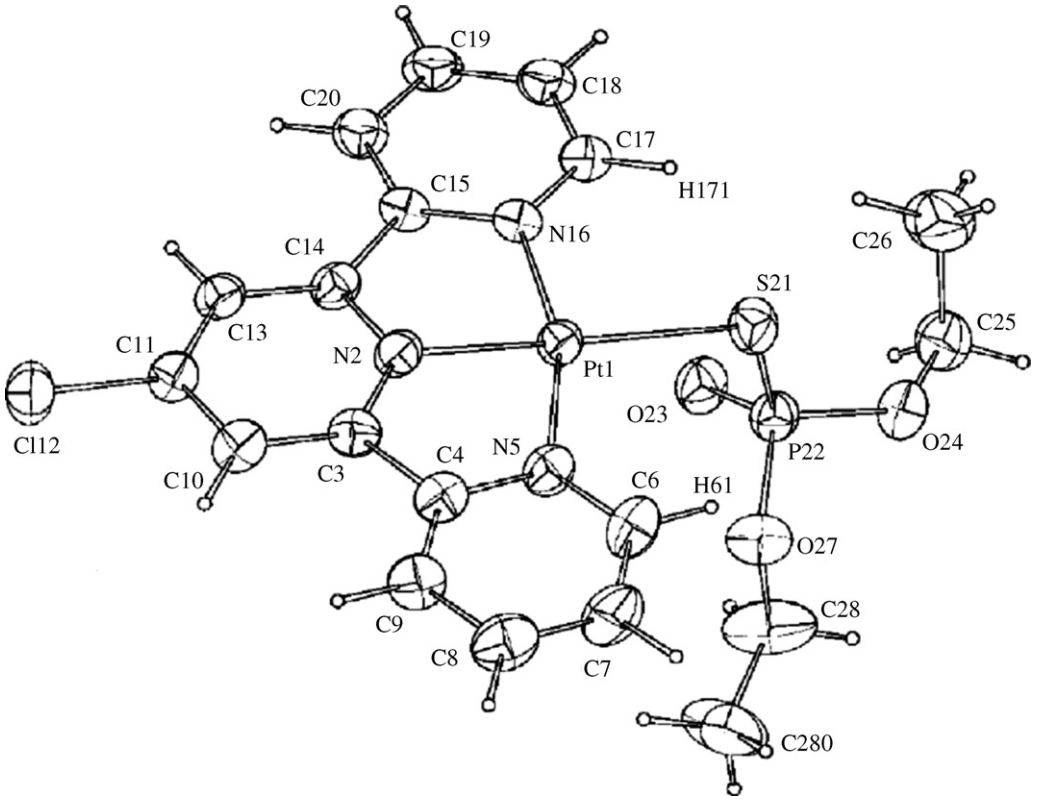

Fig. 13. Crystal structure of the diethylphosphinothioate complex cation $[Pt(Clterpy)\{SP(O)(OEt)_2\}]^{+}$; from Ref. [58] (reproduced by permission of The International Union of Crystallography).

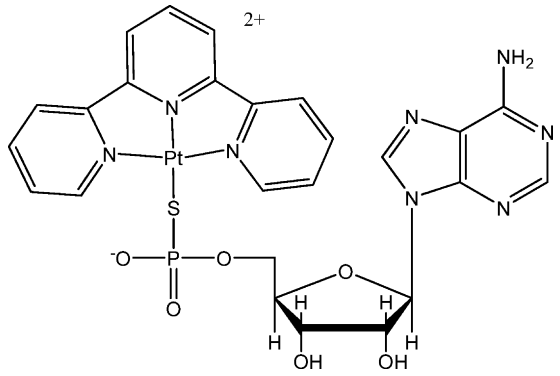

Fig. 14. S-bound platination of $[Pt(terpy)]^{2+}$ to adenosine monophosphorothioate (AMPS).

the binding of $[Pt(terpy)Cl]^{+}$ to yeast tRNA modified to have two phosphorothioate groups incorporated into the C–C–A terminus [56]. Platination of the two phosphorothioate groups on adjacent residues is complete when $r_f > 2$. At a lower concentration ratio, binding is not quantitative. The reaction of $[Pt(terpy)Cl]^{+}$ with the phosphorothioate-derivatized dinucleotide d(Tp(S)T) results in rapid (<30 min) formation of Pt–S bound diastereomers, as indicated by sets of two ^{195}Pt and ^{31}P NMR signals [57]. The diethylphosphinothioate complex cation $[Pt(Clterpy)\{SP(O)(OEt)_2\}]^{+}$ has been prepared and characterized crystallographically (Fig. 14) [58].

The ability of $[Pt(terpy)]^{2+}$ to bind to phosphate groups has been implied, but not directly observed [51].

2.5. Nucleic acid cleavage

An early report that interaction of $[Pt(terpy)Cl]^{+}$ with circular closed DNA from bacteriophage PM2 results in nicking of the supercoiled helix [17] has been followed by more recent work by several research groups on DNA cleavage by related complexes.

A novel DNA cleavage agent synthesized in the Kostić laboratory consists of an arginine-bridged Pt(II) terpy dimer attached to an FeEDTA unit [42]. Nuclease activity of $[\{Pt(terpy)\}_2Arg\text{-}EDTAFe]^{+}$ on supercoiled plasmid DNA produces nicked circular DNA and then linear DNA, indicating sequential single-stand cleavage steps. Control experiments using model compounds such as $[\{Pt(terpy)\}_2Arg\text{-}EDTA]^{+}$, methyl-guanine bridged dimer $[\{Pt(terpy)\}_2MeGua]^{3+}$, $[Fe(EDTA)]^{2-}$ indicated that efficient cleavage requires both the Pt(II) terpy dimer for DNA binding and the FeEDTA unit for hydroxyl radical production.

Investigations by Thorp and co-workers explored how binding of the $[Pt(terpy)(HET)]^{+}$ to DNA and RNA affects oxidative cleavage by a redox-active oxoruthenium(IV) complexes [59]. Preferential binding of platinum intercalator to the bulge site in the hairpin loop of TAR DNA results in structural changes within the loop.

Le Sech and co-workers investigated enhancement of single-strand and double-strand breaks in dry films of DNA upon X-ray excitation of inner-shell Pt absorption band of intercalated $[Pt(terpy)Cl]^{+}$ [60]. Subsequent work explored analogous cleavage reactions for DNA in solution [61] and showed that, as with the dry film studies, platinated DNA was cleaved approximately twice as much as unplatinated DNA. However, the effect of DMSO as a solution radical scavenger and studies of variable wavelength excitation led researchers to conclude that hydroxyl radical formation is the major cleavage mechanism. Applications to cancer therapy were discussed. In related work using irradiation by fast He^{2+}, C^{6+} and Fe^{26+} ions, the amount of both single-strand and double-strand breaks was found to increase linearly with the loading of $[Pt(terpy)Cl]^{+}$ into DNA samples [62].

3. Biological activity

Because of the binding to nucleic acids, Pt(II) terpy complexes have the ability or potential to serve as anti-cancer [63,64], antibacterial [65], and anti-parasitic [66] drugs. Although summarized in this section, the exact mechanisms are not known in some cases, and may involve protein binding (see Section 4) or membrane binding.

A report by Seto and Tomasz in 1977 described an *in vivo* use of "platinum red" (presumably [Pt(terpy)Cl]Cl) and several other DNA intercalating agents to inhibit genetic recombination in pneomococci bacteria [65].

The first report on the anti-cancer activity of Pt(II) terpy metallointercalators came from McFadyen et al., who studied a series of complexes the type $[Pt(terpy)(SPhR)]^{+}$ (with R = H, 2-OMe, 3-OMe, 4-OMe, 4-NO_2, 4-F, 4-Cl, 4-Br, 4-Me, 4-NH_3^{+}) along with $[Pt(terpy)Cl]^{+}$ and $[Pt(terpy)(1\text{-thionaphtholate})]^{+}$ for their ability to inhibit the growth of L1210 murine leukemia cells in culture [16]. All of the Pt(II) terpy complexes are effective growth inhibitors, with IC_{50} concentration values (the concentration of drug needed to inhibit cell growth by 50%) in the 4–13 μM range, except for the $[Pt(terpy)(SPhNH_3)]^{2+}$ dication (IC_{50} = 32 μM) and the labile chloro complex cation $[Pt(terpy)Cl]^{+}$ and (IC_{50} = 450 μM). The related complex $[Pt(terpy)(SC_4H_9)]^{+}$ (IC_{50} = 14 μM) is also a highly effective inhibitor [19]. Inhibition by the thiol complexes is rapid and results in extensive cell lysis, indicating that the primary role of the drugs may be on the cell membrane rather than DNA. The complex cation $[Pt(terpy)(SPh)]^{+}$ displays no inhibition on the leukemia cells in mice and was found to be toxic at dose levels of 5 mg/kg per day. Related dimers of the type $[(terpy)PtS(CH_2)_nSPt(terpy)]^{2+}$ (n = 4–10) are nearly twice as effective (IC_{50} = 2–5 μM) as analogous thiol monomers, but effectiveness does not vary with the bridging thiol chain length [19].

Lowe et al. investigated a large series of Pt(II) terpy complex cations on in vitro cytotoxicity against five human ovarian carcinoma cell lines, including two resistant to cisplatin and one resistant to doxorubicin, and found important effects of structure of the platinum drugs on activity [64]. While complex cations $[Pt(terpy)Cl]^{+}$ and $[Pt(terpy)(H_2O)]^{2+}$ are known to bind to DNA much faster than complexes having X = picoline, they are not more cytotoxic, suggesting that the rate of platination is not the most significant determinant of cytotoxicity. Variation among X = pyridine derivatives had little effect on IC_{50} values, but inclusion of a 4′-chloro substituent on the terpy ligand increased cytotoxicity. Regarding bis-intercalators, one dinuclear complex having a rigid and extended X ligand bridge showed the highest efficacy (exceeding that of cisplatin), while a dinuclear complex having bridged terpy ligands showed low activity. Interesting, even the nature of the counter-ion in the $Pt(terpy)^{n+}$ salts appears to affect anti-tumor activity.

Several Pt(II) terpy complexes containing various thioalkylcarborane ligands (one shown in Fig. 15) are cytotoxic [29,27,67,68] Studies using cisplatin-sensitive human ovarian cancer cell lines and a cisplatin-resistant variant cell line yielded similar IC_{50} values, suggesting a cytotoxicity mechanism that differs from that for cisplatin. Complexes in the series differed somewhat in their cytotoxicity, with results suggesting that differences in solubility may be controlling anti-tumor activity [68]. Related dinuclear complexes, containing two $[Pt(terpy)]^{2+}$ units arranged in different geometries about the carborane center, have also been prepared and one isomer displays greater cytotoxicity against L1210 murine leukaema cells than does cisplatin [29]. The likely mechanism of action is intercalation, but may also involve binding to proteins and enzyme inhibition (see Section 4) or lysis following binding into cell membranes. The authors highlight that complexes of this type may be well-suited for use in Boron Neutron Capture Therapy, as the water-solubility and

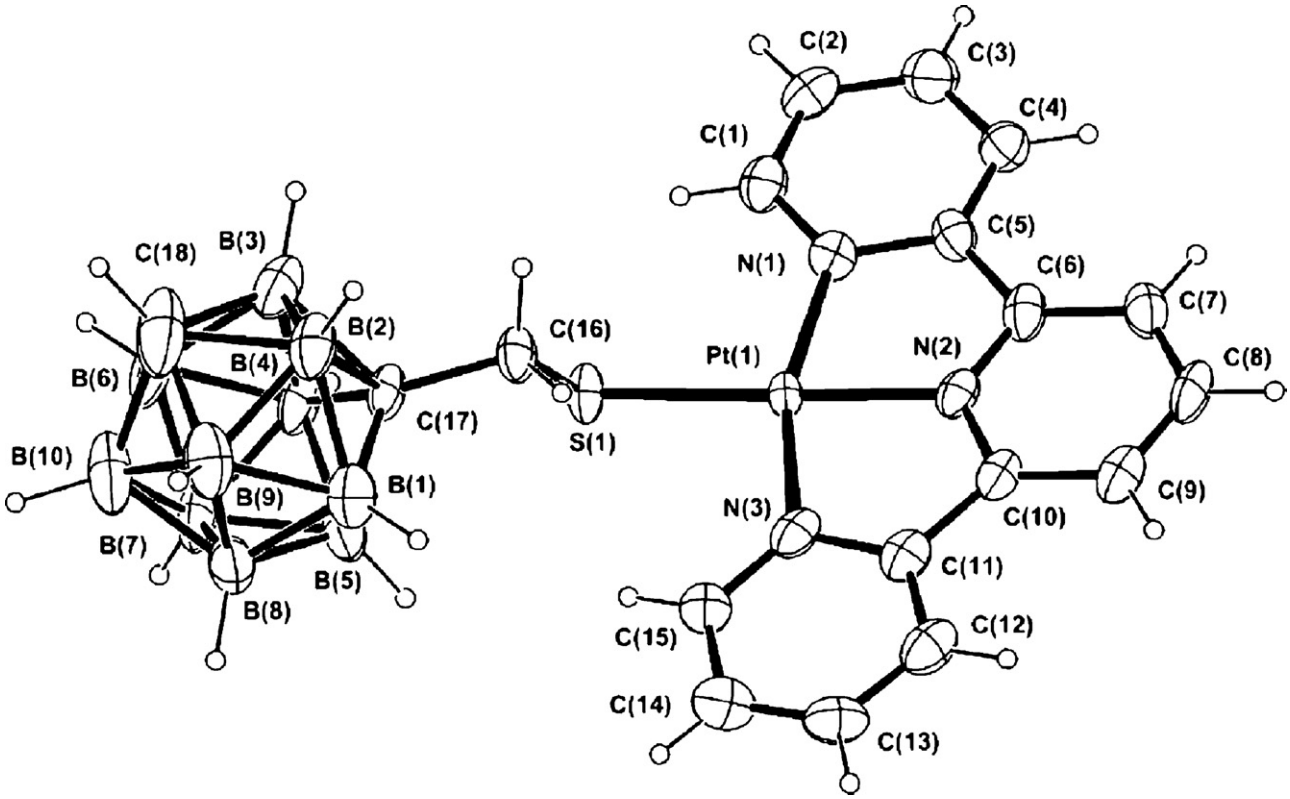

Fig. 15. Crystal structure of the carborane derivatized Pt(II) terpy complex cation $[Pt(terpy)(SCH_2C_2B_{10}H_{11})]^+$; from Ref. [68] (reproduced by permission of The American Chemical Society).

potential for intercalation by the $[Pt(terpy)]^{2+}$ unit serves as means to deliver a boron-rich drug to a tumor. Another thiolate complex $[Pt(terpy)(8\text{-thiotheophylline})]^+$ displays weak inhibition of the T2 human cancer cell line, well below that of cisplatin [69].

In an effort to develop effective multiple drug regimens for the treatment of cancer, Teicher and co-workers reported that $[Pt(terpy)Cl]^+$ displays a moderate degree of inhibition of the recovery of human squamous head and neck carcinoma cells following treatment with the anti-cancer drug bleomycin [70].

Che and co-workers have reported one a series of seven Pt(II) terpy complex cations having X = glycosylated acetylide ligand that bind to DNA [28]. The glycosylated acetylide ligand provide the complexes with stability towards ligands solvolysis common to related systems having $X = Cl^-$, while enhancing their water solubility. Studies of the effect of these drugs on five different human cancer cell lines showed that several of these new Pt(II) terpy complexes possess cytotoxicities higher than that of cisplatin.

A series of 30 complexes of the type $[Pt(Yterpy)X]^{n+}$ ($n = 1$ or 2) were tested for antiparasitic activity against three hemflagellate protozoa [66]. While many of the compounds were highly effective drugs, a mechanism of action was not established; DNA intercalation seems likely for compounds known to be substitutionally inert, and X ligand displacement followed by either covalent binding to DNA or to enzyme functional groups (Section 4) was proposed. In addition, the relative effectiveness of the Pt(II) terpy drugs varied across the three parasites.

4. Interaction and reactivity with amino acids, peptides and proteins

Coordination compounds play an important role as reagents for the study of protein structure and function. In particular, members of a growing family of Pt(II) terpy complexes possess several properties to aid investigations of their interactions with amino acids and proteins: (1) a large nucleus to serve as a tag in electron microscopy or scattering atom in X-ray crystallography of proteins, (2) selective reactivity with specific amino acid residues for investigations of enzyme active sites and applications as drugs, (3) luminescence that is sensitive to microenvironment for use in studies of protein folding, and (4) facile ground-state and excited-state redox reactions for studies of electron transfer and energy transfer in proteins.

4.1. Binding to amino acids and homologs

To understand the binding of Pt(II) terpy complexes to proteins, research efforts have focused on identifying their reactivity with individual amino acids. Complexes of the type $[Pt(Yterpy)X]^{n+}$ having labile X ligands can undergo ligand substitution reactions involving specific donor atoms of the side chains of amino acids: the S donor atom of cysteine and the N donors atom in imidazole rings (histidine and imidazole), guanidyl groups (arginine), and amine groups (glycine).

4.1.1. Cysteine and other thiols

As with many other thiols, the side chain of cysteine (Cys) reacts rapidly with $[Pt(terpy)Cl]^+$ to displace chloride and coordinate via its sulfur atom [7]. Lippard and co-workers first reported the preparation and identification of the complex $[Pt(terpy)Cys]^+$ [17], while a later report by Ratilla et al. described the observation of an immediate color change upon mixing equimolar (1–5 mM) amounts of platinum and cysteine, homocysteine and reduced glutathione [71,72]. These thiols react even in neutral and weakly acidic solution, in which the thiol exists mostly in the protonated form ($pK_a = 8.3$).

In contrast, no members of a series of thioethers (DL-methionine, *N*-acetyl-DL-methionine, *N*-acetyl-L-methionine amide, L-

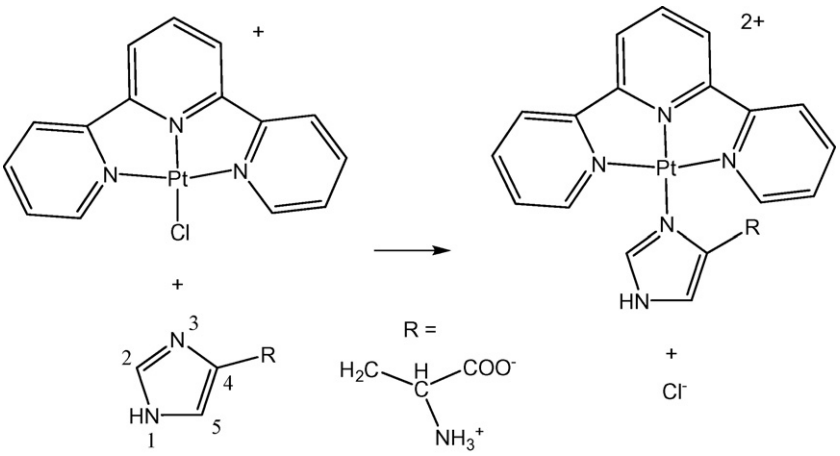

Fig. 16. Reaction of $[Pt(terpy)Cl]^+$ with histidine (His) to form $[Pt(terpy)His]^{2+}$.

methionine methyl ester hydrochloride, *S*-methyl-L-cysteine) are reactive toward chloride displacement in $[Pt(terpy)Cl]^+$ [71]. Disulfides such as cystine and oxidized glutathione are also unreactive. Ratilla et al. attribute this lack of reactivity primarily to steric effects and secondarily to differences in nucleophilicity between thiols/thiolates and thioethers/disulfides [71]. Supporting this, the authors present computational results for a model complex $[Pt(terpy)SMe_2]^{2+}$, showing contact between the methyl groups of the thioether with the hydrogen atoms in the C^6 position of the terpy ligand. A follow-up study involving other tridentate ligands in place of terpy confirmed that the reactivity of nucleophilic thioether towards Pt(II) is limited by steric effect [73]. While a report by Murienik and Bidani mentions isolating a product from the reaction of $[Pt(terpy)Cl]^+$ with tetrahydrothiophene [74], this thioether would be expected to possess less steric hindrance in the coordination plane than the biochemical sulfur compounds mentioned above.

Electron spray ionization of a 1.5×10^{-6} M solution of [Pt(terpy)Cl]Cl(aq) with a 10 M excess of cysteine results in the formation of $[Pt(terpy)Cys]^+$ in high yield [75]. Similar results are obtained using *N*-methylcysteine (MeCys), but the reaction with *S*-methylcysteine produces $[Pt(terpy)(MeCys)]^+$ only in low yield. Fragmentation pathways of the product, detected using collision-induced dissociation tandem mass spectrometry, supported assigning the complex structure as having an S-bound amino acid.

In a pH 6 solution, $[Pt(terpy)Cys]^{2+}$ can form from the reaction of $[Pt(terpy)guanosine\text{-}N^7]^{2+}$ with cysteine. Although the product is inert toward ligand substitution by guanosine-5′-monophosphate, inosine or inosine-5′-monophosphate, sulfur donor ligands diethyldithiocarbamate, thiosulfate and thiourea are capable of slowly displacing cysteine [51,52].

4.1.2. Histidine and other imidazoles

Another primary mode of reaction of $[Pt(terpy)Cl]^+$ with amino acids is through chloride ligand displacement by nitrogen atom donors [7]. The reactions of [Pt(terpy)Cl]Cl with histidine (His) and homologs imidazole (Im) and N^{α}-acetyl-L-histidine proceed more slowly than the reactions using cysteine and related thiols, occurring over the course of an hour for solutions of 5 mM reactants [71]. Products of these reactions initially were characterized as having the imidazole ring bound to platinum via the imine nitrogen atom N^3 (Fig. 16) rather than through the pyrrole nitrogen atom N^1, which is protonated ($pK_a = 14.5$) [71]. Supporting this is the observation that the immine nitrogen ($pK_a = 6.0$–6.5) can be protonated in weakly acidic solutions, resulting in a slower reaction rate with platinum. In a subsequent study, Appelton et al. used ^1H and ^{195}Pt NMR spectroscopies to identify both major and minor reaction products, corresponding to linkage isomers of the histidine or *N*-acetylhistidine ligand [76]. In addition, they point out the reaction of $[Pt(terpy)Cl]^+$ with *N*-acetylhistidine reaches equilibrium, not completion at pH ≤ 5. Coordination of a specific imidazole ligand results in UV–vis absorption changes that are diagnostic for identifying which amino acids are platinated in peptides (see below) [71].

The reaction of 1-methylimidazole with $[Pt(terpy)Cl]^+$ in a pH 9 solution also affords a product in which the 1-methylimidazole ligand is coordinated through the N^3 position [77]. In contrast, a similar reaction using 1-methyltetrazole results in deprotonation and unusual coordination of the ligand through the C^5

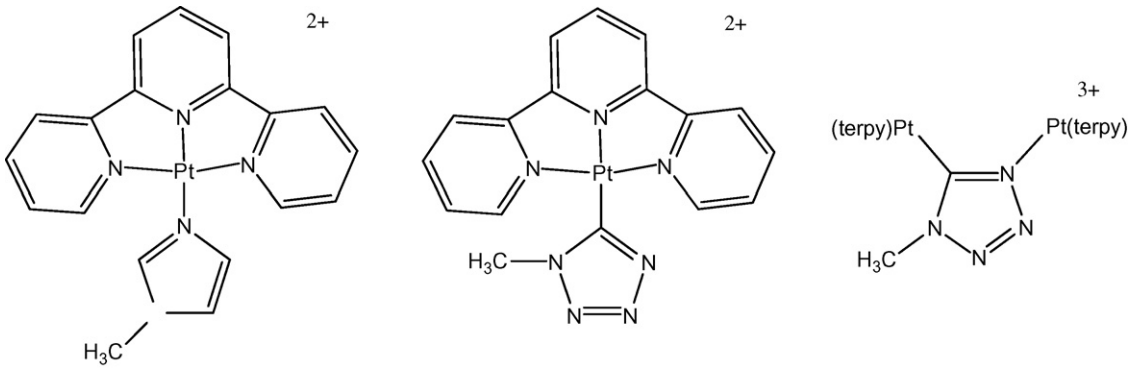

Fig. 17. Structures of 1-methylazole complex cations $[Pt(terpy)(1\text{-methylimidazole})]^{2+}$, $[Pt(terpy)(1\text{-methyltetrazolate})]^{2+}$, and $[\{Pt(terpy)\}_2(1\text{-methyltetrazolate})]^{3+}$.

carbon, while at pH 2.5, a dinuclear complex cation [{Pt(terpy)}$_2$(1-methyltetrazole)]$^+$ forms in which coordination occurs through the N^4 and C^5 positions (Fig. 17).

Kinetics of the ligand-substitution reaction of [Pt(terpy)Cl]$^+$ with 100-fold excess of amino acid His, Im or Cys follows a first order rate law. Rate constants depend on the nature of the amino acid, with cysteine ($k_{obs} = 1.3 \times 10^{-2}$ s^{-1}) reacting over 1500 times faster than histidine ($k_{obs} = 8.5 \times 10^{-5}$ s^{-1}) [78]. A competitive kinetics experiment using equimolar [Pt(terpy)Cl]$^+$, cysteine and histidine yields only [Pt(terpy)Cys]$^+$ as the product [72]. While the histidine complex cation [Pt(terpy)His]$^{2+}$ is stable in aqueous solution, even at pH 3, His can be displaced by thiols, including cysteine in its deprotonated or protonate form. However, [Pt(terpy)His]$^{2+}$ is inert with respect to substitution by organomecury reagents, including mercurated cysteine. This relative reactivity has important consequences for protein labeling (see below) [78]. The histidine ligand in [Pt(terpy)His]$^{2+}$ can also be displaced using one equivalent of thiocyanate or thiourea or 100 equivalents of bromide. In contrast, the cysteine ligand in [Pt(terpy)Cys]$^+$ is only partially displaced when 10 equivalents of thiocyanate or thiourea is used [72].

4.1.3. Arginine and other guanidines

The amino acid arginine and related guanidine ligands of the type –N=C(NH_2)(NHR) (guanidine, methylguanidine, *N*-acetylarginine and canavanine) react slowly with [Pt(terpy)Cl]$^+$ upon heating at pH 7–9 yielding two types of complex cations [79,80]. Yellow mononuclear complex cations of the type [Pt(terpy)L]$^{2+}$ have guanidine coordination to Pt(II) through an imine nitrogen atom, with two possible tautomers (Fig. 18). In red dinuclear complex cations of the type [{Pt(terpy)}$_2$L]$^{3+}$, guanidine serves as a bridging ligand, with coordination to the Pt(II) ions through the amine nitrogen atoms; this was the first example of a bridging guanidine ligand in the literature [80]. Two types of [{Pt(terpy)}$_2$L]$^{3+}$ structures co-exist in the solid state for L = canavanine, distinguished by different nitrogen atom donors (Fig. 19). The monometallic complexes form with and convert to the bimetallic complexes, which can also be formed exclusively with prolonged heating of a 2:1 ratio of [Pt(terpy)Cl]Cl and guanidine ligand.

The reactivity of [Pt(terpy)Cl]$^+$ increases for guanidine ligands with lower basicity (e.g. canavanine with pK_a = 7.0) and increases at higher solution pH (though below pH 9.5 to limit displacement of chloride by hydroxide) [80]. Other amino acids bearing side chains with heteroatoms (Lys, Trp, Asp, Asn, Glu, Gln, Pro, Thr, Ser, Tyr and Met) are not known to form Pt(II) terpy complexes [79]. Specifically, amino or carboxylate groups of amino acids do not appear to serve as ligands to displace chloride in [Pt(terpy)Cl]$^+$.

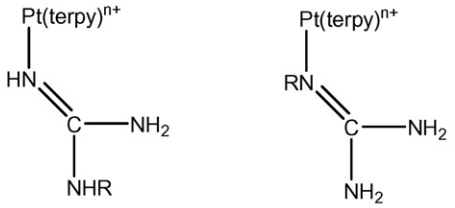

R = H (guanidine); n = 2
R = CH_3 (methylguanidine); n = 2
R = $(CH_2)_3CH(NH_3^+)(COO^-)$ (argenine); n = 2
R = $O(CH_2)_2CH[CH_3C(O)NH](COO^-)$ (acetylargenine); n = 1
R = $O(CH_2)_3CH(NH_3^+)(COO^-)$ (canavanine); n = 2

Fig. 18. Two tautomers proposed for mononuclear [Pt(terpy)L]$^{n+}$ complex cations having guanidine ligands.

4.1.4. Glycine

Although [Pt(terpy)Cl]$^+$ does not react with glycine in solution, electron spray ionization of a 1.5×10^{-6} M solution of [Pt(terpy)Cl]Cl (*aq*) with a 30–50 M excess of glycine, *N*-methylglycine or *O*-methylglycine results in the formation of small amounts of [Pt(terpy)Gly]$^{2+}$ and [Pt(terpy)Gly]$^+$ in the gas phase [75]. Fragmentation pathways of these products, detected using collision-induced dissociation tandem mass spectrometry, supported assigning the complex structure as having a N-bound amino acid.

4.2. Binding to peptides

4.2.1. Cysteine-containing peptides

The tripeptide γ-Glu-*Cys*-Gly, glutathione, is the most abundant non-protein thiol in eukaryotic cells and serves as an antioxidant because of its free thiol group. The formation of metal–thiol complexes is an important part of the mechanism for detoxification of heavy metals such as Hg^{2+} and Cd^{2+} in mammals and is a competing side reaction in the therapeutic use of cisplatin anti-cancer drugs.

The high reactivity of [Pt(terpy)Cl]$^+$ with thiols [7] allows for rapid labeling of peptides and proteins through the formation of covalent Pt–S bonds with thiol side chains of amino acids. First reported by Kostić and co-workers, the reaction of [Pt(terpy)Cl]$^+$ with glutathione (GSH) at pH 7 yields [Pt(terpy)GS] [72,78,81]. The product has been described as having a neutral [78], +1 [72,82–84], or +2 [81,85] charge in various reports, presumably reflecting the degree of ionization of the two carboxylate groups of the glutathione ligand for particular solution pH. Under conditions of excess glutathione, the chloride substitution reaction follows first order kinetics [72], and a Job's plot indicates a 1:1 binding of platinum and the tripeptide [78,85]. No glycine hydrolysis product is observed to form from this solution, even after weeks. In contrast, [Pt(terpy)Cl]$^+$ does not react with the larger *S*-methylglutathione, presumably due to a steric effect of the terpy *ortho* hydrogens in preventing the bulky thioether from displacing chloride [81].

Juranić et al. presented results of a detailed investigation of the conformation of [Pt(terpy)GS]$^+$ in solution using a combination of two-dimensional cross-relaxation ^{1}H NMR spectroscopy with molecular-mechanics and molecular-dynamics calculations [82]. In a DMF/water mixture at −15 °C, the complex has a conformation in which the glutamyl residue of the glutathione ligand lies over and within 3.5 Å of one of the terminal terpyridine pyridyl rings (Fig. 20). This hydrophobic interaction compresses the glutathione structure from that observed for the free tripeptide. Further characterization of [Pt(terpy)GS]$^+$ came from a study comparing the infrared and Raman spectra of the complex with calculated normal modes from an optimized structure [83].

While most [Pt(terpy)SR]$^+$ complexes are reported to be thermodynamically stable for several days in water, some examples of reactivity of the Pt–S bond in [Pt(terpy)GS]$^+$ have been found. Lowe and co-workers observed displacement of glutathione in [Pt(Clterpy)GS]$^+$ by other thiols [84]. In the presence of one equivalent of $CuCl_2$(aq) in neutral phosphate buffer, the Pt–S bond in [Pt(terpy)GS]$^+$ dissociates to yield [Pt(terpy)Cl]$^+$ [85]. Insight into this mechanism came from evidence of an S-bridged heterodinuclear complex forming between [Pt(terpy)GS]$^+$ and the Cu(II) ion at pH < 7 and coordination of the amide nitrogen of GS to Cu(II) at pH ≥ 7. A proposed transition state structure is given in Fig. 21.

The cyclic metallopeptides cyclo[Gly-L-*Cys*{Pt(terpy)}]$_n$Cl$_n$ (n = 3, 4) were the first example of a liquid-phase synthesis of such supramolecular structures from a linear metallopeptide (Fig. 22) [86]. Through rapid reaction with the cysteine thiols, [Pt(terpy)Cl]$^+$ promotes peptide cyclization and can also act as a protecting group by subsequently being removed through treatment with tetrafluoroacetic acid. The cyclic metallopeptides, which can also

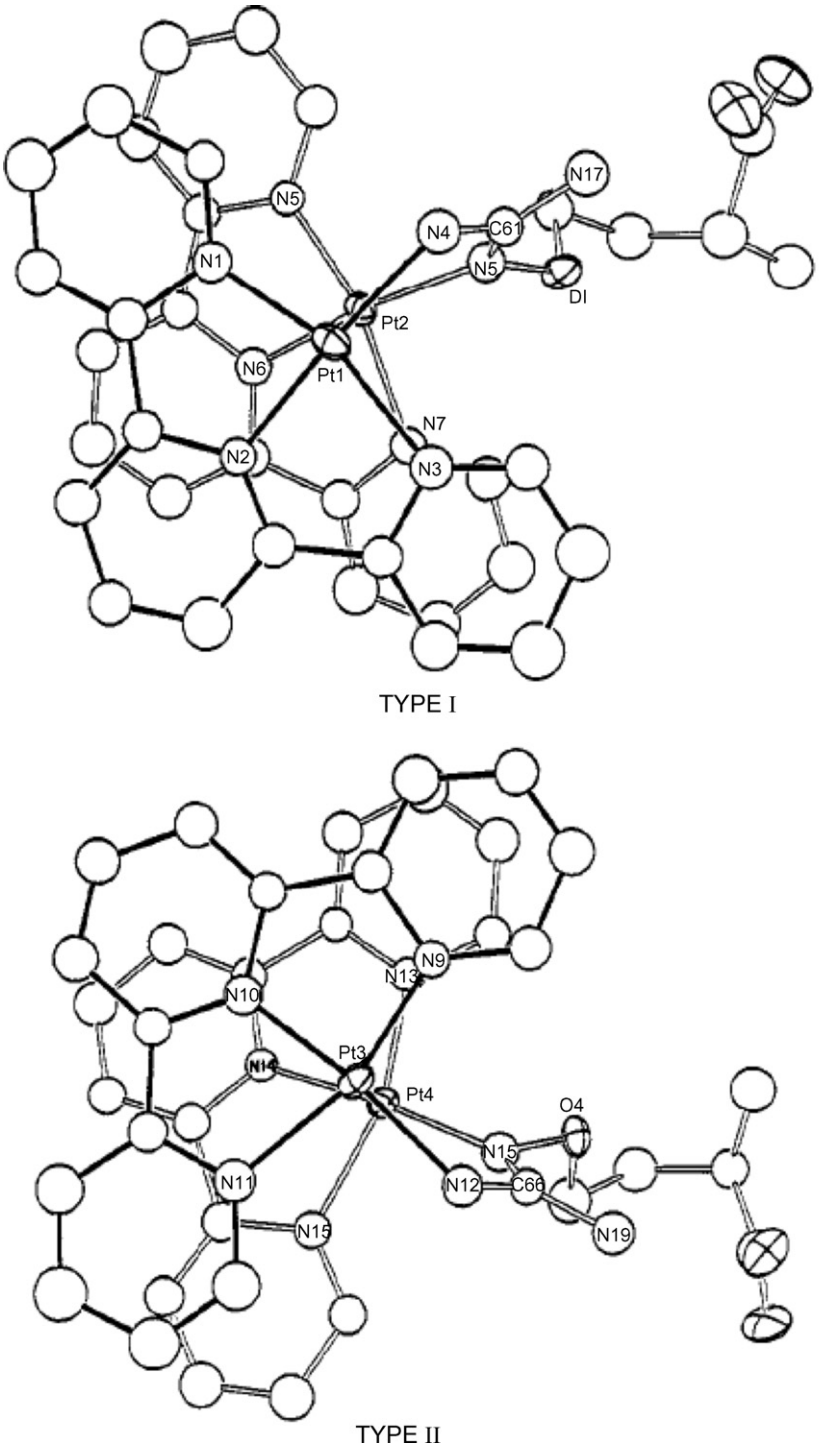

Fig. 19. Structures of two types of dinuclear $[Pt(terpy)Can]^{3+}$ complex cations, differing in their mode of coordination to canavanine; from Ref. [80] (reproduced by permission of The American Chemical Society).

serve as selective anion receptors for benzene tricarboxylates, have been characterized by high-resolution ESI-TOF mass spectrometry and ^{1}H NMR spectroscopy [87].

4.2.2. Histidine-containing peptides

Kostić and co-workers first reported that reactions of $[Pt(terpy)Cl]^+$ with a variety of small histidine-containing peptides, including L-histidyl-L-histidine (His-His), L-histidyl-L-lysine (His-Lys), and glycine-L-histidyl-L-glysine (Gly-His-Gly), resulted in platination of histidine residues [71]. Relative intensities of the UV–vis bands at 342 and 328 nm are diagnostic for which ligand binds to platinum, and Job's plots indicate that only one amino acid binds platinum [71,78].

The ligand substitution reaction of $[Pt(terpy)Cl]^+$ with 100-fold excess of various tripeptides follows first order kinetics, with relative rate constants much higher for those containing cysteine than for histidine. Consequently, in a competition between equimolar γ-Glu-Cys-Gly and Gly-His-Gly, $[Pt(terpy)Cl]^+$ reacts exclusively with the cysteine, even though there is a higher amount of deprotonated histidine than deprotonated cysteine at pH 7 [78].

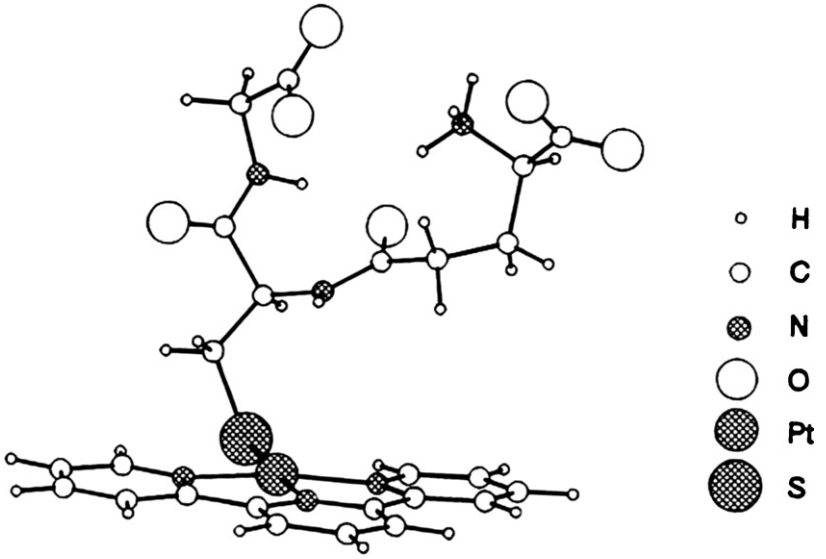

Fig. 20. Structure of $[Pt(terpy)GS]^+$ as determined from 2D NMR spectroscopy; from Ref. [82] (reproduced by permission of The American Chemical Society).

4.2.3. Poly(glutamic acid)

Scolaro et al. reported that the reaction of [Pt(terpy)Me]Cl with α-helical poly(glutamic acid) yielded "the first example of a supramolecular aggregate formed by an organometallic platinum(II) complex [43]." A sequence of changes to the CD spectrum of the solution mixture at pH 4.5 supported a mechanism in which the platinum complex cation initially forms a low-ordered adduct through electrostatic attraction to carboxylate groups. Next, a series of three conformational rearrangements leads to a final organized assembly in which $[Pt(terpy)Me]^+$ chromophores are strongly coupled and postulated to be arranged into an α-helix by the polypeptide template. Interestingly, the use of the complex cations $[Pt(terpy)Cl]^+$, $[Pt(terpy)Ph]^+$ and $[Pt(Phterpy)Ph]^+$ results in no interaction with poly(glutamic acid) while $[Pt(Phterpy)Me]^+$ has only weak interaction.

4.2.4. Glycine-containing peptides

Following incubation of [Pt(terpy)Cl]Cl(aq) with a 40-M excess of dipeptides glycylglycine (Gly-Gly), glycylalanine (Gly-Ala) or alanylglycine (Ala-Gly) for 3 days, peptide complex ions $[Pt(terpy)M]^{2+}$ and $[Pt(terpy)M-H]^+$ (having deprotonated carboxylate) were detected using electron spray ionization [88]. Fragmentation pathways of these two ion products differ from each other and involve the formation of several products, involving peptide bond cleavage, OH abstraction, hydride transfer with reductive elimination, and an unusual peptide rearrangement reaction.

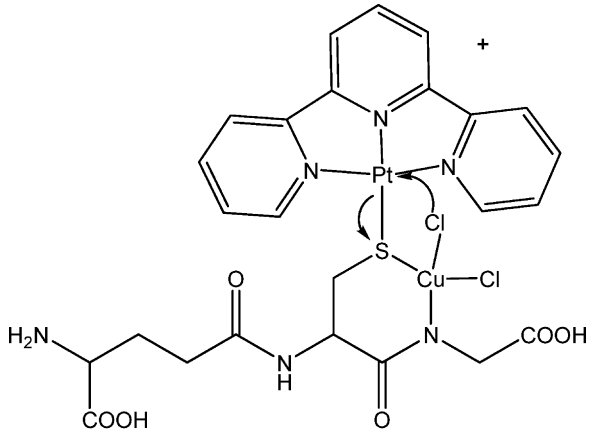

Fig. 21. A proposed transition state structure for the reaction of $[Pt(terpy)GS]^+$ with $CuCl_2$; adapted from Ref. [85].

The reaction of the Ir(I) oligopeptide complex $[(\eta^5\text{-}Me_5Cp)Ir(dppz)(S\text{-Gly-Met-OH})]$ with $[Pt(terpy)Cl]^+$ results in chloride displacement by the glycine S atom [33].

4.3. Binding to proteins

Similar to the modes of DNA binding described in Section 2, binding of $[Pt(terpy)]^{2+}$ to proteins occurs through a combination of covalent bonding to specific amino acids and non-covalent interactions in the local microenvironment of the protein structure. Investigations of the binding of Pt(II) terpy complexes to albumin, cytochrome *c*, and protease enzymes will be summarized after a few general comments about protein binding.

Kostić has pointed out that Pt(II) terpy complexes satisfy many of the criteria for an ideal label of amino acid side chains [89]. Specifically, this label: (1) reacts selectively with amino acid side chains under mild conditions, (2) is easily detected and quantified, (3) is stable but removable, and (4) is noninvasive. A general method for preparing proteins labeled with $[Pt(terpy)]^{2+}$ has been presented by Kostić [89]. Ion-exchange chromatography allows for separation of proteins having different numbers and distributions of $[Pt(terpy)]^{2+}$ labels; typically, a greater number of platinum complex cations bound to the protein results in greater retention by a cation exchange column and less by an anion exchange column. However, chromatographic separation also depends on the distribution of the platinum complex cations on the protein, as seen for different retentions for horse heart cytochrome *c* labeled at His-33 and His-26 [71].

4.3.1. Specificity of binding

As with peptides, proteins bind $[Pt(terpy)Cl]^+$ selectively at cysteine and histidine [89]. The yield of labeling a particular residue increases when the side chain is more accessible from the bulk solution, but even fully accessible cysteines are not labeled quantitatively. Because of this selectivity, the platinum reagent can serve as a probe of protein topography. Although the labeling reaction is rather slow because $[Pt(terpy)X]^+$ complex cations are kinetically inert toward ligand substitution reactions [7], the resulting labeled proteins are also stable under ordinary solution conditions, allowing for subsequent biochemical analysis such as chromatog-

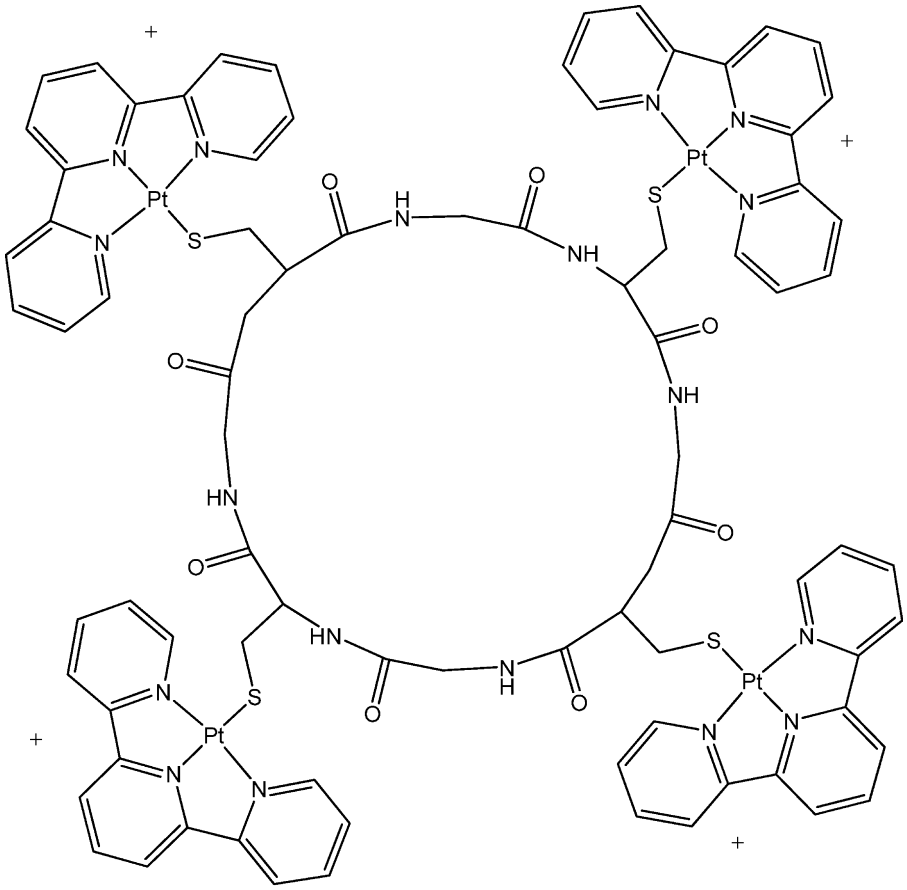

Fig. 22. Example of a cyclic metallopeptide having pendant $[Pt(terpy)]^{2+}$ units; adapted from Ref. [86].

raphy, ultrafiltration, dialysis and peptide mapping techniques. However, migration of the platinum complex cations can occur during protein denaturation or digestion, when previously inaccessible residues become available for binding. Specifically, $[Pt(terpy)]^{2+}$ can migrate from histidine residues to free cysteine residues, due to the difference in nucleophilicity of these two donor ligands. The addition of organomercury reagents for protein mapping will not affect either cysteine-bound or histidine-bound platinum cations. Removal of platinum tags from histidine residues can be accomplished by taking advantage of the relative nucleophilicity of various ligands. Bromide, iodide thiocyanate and thiourea can serve as reagents for the removal of platinated histidine [78,89].

Notably, the binding selectivity is opposite of that for $[PtCl_4]^{2-}$, which show much higher reactivity toward methionine than histidine. The terpy ligand enhances this selectivity through steric bulk to limit thioether binding and electronic effects that increase lability of the chloride ligand [71].

4.3.2. $Pt(terpy)^{2+}$ as a spectroscopic probe

Monitoring and quantifying the labeling of proteins by $[Pt(terpy)]^{2+}$ can be accomplished using UV–vis absorption spectrophotometry. All $[Pt(terpy)X]^{+}$ complexes absorb strongly in the 300–350 nm near-UV region where protein absorption is minimal. The nature of the amino acid bound to the platinum complex cation can be identified by comparison of wavelength maxima, while the microenvironment of the chromophore can be elucidated from the relative intensities of band maxima. Specifically, the ratio of absorbance at 342 nm and 328 nm increases when the chromophore is in a hydrophilic environment [90]. Difference spectroscopy, derivative absorption spectra and comparison to simulated spectra are useful methods for identifying the labeling of cysteine and/or histidine residues [89].

4.3.3. Albumin

Albumin, the most abundant plasma protein, is responsible for regulating osmotic pressure, maintaining pH, and transporting small molecules. The 66 kDa protein contains one free cysteine (Cys-34) located in an interior pocket. Ross et al. showed that the reaction of recombinant human albumin (rHA) with $[Pt(Clterpy)(pyridine\text{-}4\text{-}thione)]^{2+}$ results in release of pyridine-4-thione and binding of $[Pt(Clterpy)]^{2+}$ to Cys-34 (detected by electrospray-ionization mass spectrometry) while a Cys-34-blocked rHA shows no spectroscopic changes [84]. The reaction reaches completion after 60 min and the Pt(II) tag can be subsequently partially displaced by glutathione. Even slower reactions are observed for reactions of rHA with thiolate complexes $[Pt(Clterpy)(SR)]^{+}$ (where SR = $^{-}SCH_2CH_2OH$, $^{-}SCH_2CH_2CH_2OH$, or glutathione). The authors suggest potential for using platinated human serum albumin to deliver platinum-based chemotherapeutic drugs into tumor cells [84].

Yam and co-workers have used the luminescent complex cations $[Pt(^{t}Bu_3terpy)(C{\equiv}CPhNCS\text{-}4]^{+}$ and $[Pt(^{t}Bu_3terpy)(C{\equiv}CPhNHCOCH_2I\text{-}4]^{+}$ as labeling reagents of human serum albumin (HSA) [91]. Instead of ligand substitution chemistry and the direct platination of the protein, the isothiocyanate and iodoacetamide groups to react with primary amine and sulfhydryl groups, respectively, of HSA. Both complex cations are luminescent when bound to HSA and represent the first examples of using Pt(II) terpy complexes as luminescent protein labels.

In an attempt to make platinum-based cancer drugs more specific to the types of cells they target, some research groups have

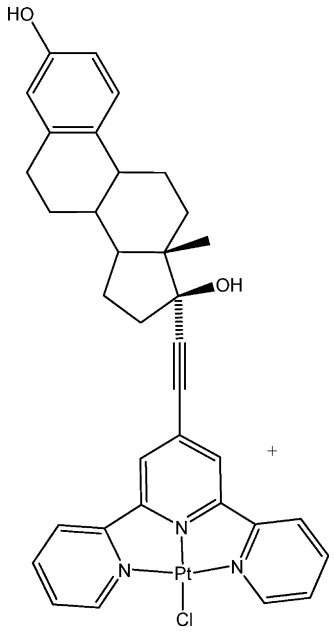

Fig. 23. An estrogen-platinum terpyridine conjugate drug, 17a-[4′-Ethynyl-2,2′:6′,2″-terpyridine]-17b-estradiol platinum(II) chloride.

constructed conjugate drugs containing platinum reagents with steroid hormones. One recent example is a Pt(II) terpy complex having a pendant estradiol group (Fig. 23), for which covalent binding to DNA, but not intercalation, is possible [92]. Relative to estradiol, binding of the conjugate drug to estrogen receptor is retained but significantly reduced, perhaps due to steric bulk of the terpy ligand and its proximity to the estrogen unit. Results of circular and linear dichroism and mass spectroscopy studies indicate that the Pt(II) terpy complex binds to DNA, HSA, and to both simultaneously. The work opens the door to other types of pendant delivery vehicles to Pt(II) terpy chemotherapeutic drugs.

4.3.4. Acetylcholinesterase

The hydrolysis of acetylcholine and other acetic acid esters is catalyzed by acetylcholinesterase (AChE) with remarkable speed. Structural investigations of this enzyme have revealed an active site having a large negative charge and the presence of remote cationic receptor binding sites which influence catalysis at the active site. Rosenberry and co-workers reported on the use of $[Pt(terpy)Cl]^+$ to label and inhibit human AChE [93]. Platination of AChE occurs upon a 1-h incubation of the enzyme with $[Pt(terpy)Cl]^+$, and unreacted platinum reagent can be separated using column chromatography. Because the enzyme contains no free thiol groups, histidine residues are the likely site for platination. A similarity of the rate constant for the reaction of 2-mercaptoethanol with platinated AChE ($k = 39 \pm 4\,M^{-1}\,s^{-1}$) and with $[Pt(terpy)(Im)]^{2+}$ ($k = 21 \pm 1\,M^{-1}\,s^{-1}$) supported an assignment of a histidine residue as the $[Pt(terpy)]^{2+}$ binding site. Results of competitive kinetics experiments using the known inhibitor ambenonium suggested that the Pt(II) terpy label resides near the active site. Trypsin digestion of the platinated enzyme and sequencing of the resulting tryptic peptides indicated that more than one His site may be labeled. Platination results in inhibition of acetylcholine hydrolysis, but not of phenyl acetate hydrolysis, suggesting that the His-440 residue of the catalytic triad was not the site of platination. Inhibition was found to increase during the incubation period and remains irreversible over at least 1–2 days, but with an inactivation rate constant that is much larger than the second order rate constant for the reaction of $[Pt(terpy)Cl]^+$ with imidazole and not proportional to the platinum reagent concentration. An analysis of variations in the His positions in the amino acid sequence for the active site gorge between several species indicated that His-280 is the likely binding site.

4.3.5. Cytochrome c

Cytochrome *c* is a heme protein involved in the electron transport chain of mitochondrial respiration. Four types of cytochrome *c*, each having similar amino acid sequence and folded structure, have been investigated for labeling with Pt(II) terpy complexes [71,78]. The binding sites for the platinum reagent were determined through analysis of difference UV–vis spectra and peptide mapping. In each case, labeling with $[Pt(terpy)]^{2+}$ does not affect the structure or redox properties of the cytochrome, as evidenced by no change in the optical, electrochemical, ESR or ^1H NMR spectroscopic properties of the heme environment. His-18 remains axially bound to the heme and unavailable for platinum labeling.

At pH 5, $[Pt(terpy)Cl]^+$ selectively labels histidine sites of cytochrome *c*. Binding of $[Pt(terpy)]^{2+}$ to tuna heart cytochrome *c* (which contains only one available histidine and no cysteine) occurs exclusively at His-26 [71]. For the reaction of $[Pt(terpy)Cl]^+$ with horse heart cytochrome *c* (which contains two available histidine residues and lacks free cysteine), products include both single and double platinum binding at residues His-33 and/or His-26. Platination of His-33, which is found in a hydrophilic site in the protein exterior is preferred over binding to His-26, which lies in a hydrophobic pocket [71]. With cytochrome *c* from *Candida krusei*, reactions with the two available and surface-exposed histidine residues (His-33 and His-39) results in a mixture of a minor doubly-labeled product, and two major singly-labeled products in equal yield [78]. Cytochrome *c* from Baker's yeast contains three available histidine residues in addition to a reactive cysteine. Reaction with $[Pt(terpy)Cl]^+$ results in three major products singly-labeled at His-39, His-33 and Cys-102, and three minor products doubly-labeled at combinations of two of the same three residues [78]. The His-26 site cannot compete with the other available binding sites in this protein and remains unlabeled. Interestingly, the yield of the cysteine-labeled product is lower than the two histidine-labeled products, despite high reactivity of the cysteine toward organic reagents and the high preference of $[Pt(terpy)Cl]^+$ for cysteine over histidine. This study demonstrated both that Cys-102 is inaccessible from solution and that $[Pt(terpy)Cl]^+$ serves as a non-invasive labeling reagent.

At pH 7, additional reactivity can occur for tuna heart and horse heart cytochrome *c*, involving platinum labeling of a barely surface-exposed arginine residue (Arg-91) in addition to the histidine residues mentioned above [79]. Due to the location of Arg-91 in the protein structure, the guanidine group possesses an unusually low pK_a value which enhances ligation to Pt(II). A report by Jackman et al. on the reaction of [Pt(terpy)Cl]Cl with horse heart cytochrome *c* mentions labeling only at the His-33 site, and subsequent inhibition of the reaction of the protein with the histidine label diethylpyrocarbonate [94].

Labeling experiments have become an established tool for cytochrome *c* modification. A $[Pt(terpy)]^{2+}$ tag on horse heart cytochrome *c* results in a large increase in the quantum yield for photoreduction of the heme [95]. The conformers adopted by horse heart cytochrome *c* in 30% acetonitrile were identified by comparison of the ^1H NMR spectra of the unlabeled protein with that doubly-labeled by $[Pt(terpy)]^{2+}$ [96]. A student laboratory experiment has been developed in which the products of the reaction of [Pt(terpy)Cl]Cl with horse heart cytochrome *c* are studied using HPLC and UV–vis spectroscopy [97].

4.3.6. Proteolytic enzymes

Brothers and Kostić reported that the reaction of $[Pt(terpy)Cl]^+$ with the serine protease enzymes α-lytic protease or α-chymotrypsin results in platinum labeling of His-57 in the former and His-57 and His-40 in the later [90]. All cysteine residues in these enzymes form disulfide and are therefore unavailable to serve as ligands to platinum. The histidine residues are found on the protein surface and His-57 is part of the catalytic triad of the active site. UV–vis absorption studies indicate that the platinum tag remains exposed to water, even when coordinated to the hydrophobic active site. Platination of α-chymotrypsin results in a decreased catalytic activity compared to the unlabeled enzyme, with esterase activity toward amino acid substrates only 2% that of the native value and hydrolysis of *N*-succinyl-AAPF-*p*-nitroanilide 25% of the native rate. Catalytic activity of α-lytic protease is also reduced upon platinum labeling. The incomplete inhibition for both labeled proteins indicates that platination of the active site does not entirely inactive these enzymes, and the authors address effects that the platinum reagent may have on the charge, structure and hydration of the active site. This study highlights the unique ways in which $[Pt(terpy)Cl]^+$ differs from organic histidine labels.

Among the 212 residues of papain, a proteolytic enzyme from papaya latex, three are capable of binding platinum: Cys-25 and His-159, which are part of the catalytic triad at the active site, and a distant His-81 [72]. Reaction with one equivalent of $[Pt(terpy)Cl]^+$ results only in labeling of Cys-25, with a bimolecular rate constant ($k = 21.3\ M^{-1}\ s^{-1}$) that is close to that for the reaction with Cys. Reaction with 50-fold excess of $[Pt(terpy)Cl]^+$ results in a doubly-labeled product, with platination at Cys-25 and His-81, as the N-atom donor in His-159 points toward the protein interior and is also too close to Cys-25 for a second platinum complex to bind. In contrast to the reactivity of $[Pt(terpy)His]^{2+}$, the histidine-bound $[Pt(terpy)_2]^{2+}$ *cannot* be selectively removed from the doubly-labeled papain using one equivalent of thiocyanate or thiourea, but can be using successive treatments of 100 equivalents of bromide followed by dialysis. The cysteine-bound platinum reagent is only partially displaced when 10 equivalents of thiocyanate or thiourea is used. These results were the first example of selective removal of a metal complex tag from a protein.

A study by Lind et al. demonstrated that treatment of the serine protease plasmin with $[Pt(terpy)Cl]^+$ results in inhibition of the enzymatic activity, presumably due to binding at the His-630 residue of the active site [98]. This platinated enzyme was then used to demonstrate the role of Cu(II)/ascorbate oxidation of this residue in the chemistry associated with fibrin clot formation.

4.3.7. Zinc finger proteins

Serving as a model for potential reactivity between Pt/DNA adducts and cysteine-rich zinc finger proteins, the reaction between $[Pt(terpy)Cl]^+$ and a Zn(II) dimer complex $[Zn(bme\text{-}dach)]_2$, where bme-dach = *N*,*N*′-bis(2-mercaptoethyl)-1,4-diazacycloheptane, involves interesting ligand scrambling to produce $[Zn(terpy)Cl]^+$ and a bimetallic complex $[Zn(bme\text{-}dach)Cl]_2Pt$ [99].

4.4. Applications as protein-binding reagents

Covalent modification of amino acid side chains is a common tool to investigate the role of specific residues in a variety of cellular processes. Possessing the characteristics of an ideal protein tag, Pt(II) terpy complexes increasingly are being studied for their application in inhibition of enzymatic activity of cellular and membrane proteins, peptide hydrolysis, and X-ray crystallography of proteins.

4.4.1. Histidine-modified photosystem II membrane proteins

The photosystem II (PSII) membrane protein of photosynthetic organisms contains the molecular components for light absorption and catalytic water splitting to produce O_2, H^+ and electrons. Seibert and co-workers have used $[Pt(terpy)]^{2+}$ in their investigations into the role of high affinity Mn-binding sites in PSII [100]. Using an assay based on detecting Mn inhibition of diphenylcarbazide photooxidation by PSII, the researchers found that $[Pt(terpy)]^{2+}$ in low concentrations (<50 μM) modifies the luminal side of the PSII membrane by binding at two His residues that normally bind Mn. At higher concentrations, $[Pt(terpy)]^{2+}$ also modifies the stromal side of the protein by binding to cysteine residues which do not bind Mn. The report also discusses competition between $[Pt(terpy)]^{2+}$ and Mn binding.

Modification of the His residues of thylakoid proteins from cyanobacteria with $[Pt(terpy)]^{2+}$ results in inhibition of the light-induced formation of an adduct between the D1 polypeptide and cytochrome *b*-559, indicating the importance of the His-252 residue in this process [101].

4.4.2. Histidine-modified pyruvate dehydrogenase kinase

Pyruvate dehydrogenase kinase (DPK) controls phosphorylation in the pyruvate dehydrogenase complex, which directs the entry of carbon in the Krebs cycle of mitrochondria. A study by Randall and co-workers describes substantial inhibition of PDK autophosphorylation following incubation with 1.6 mM $[Pt(terpy)]^{2+}$, supporting a proposal that His residues are part of the catalytic activity [102].

4.4.3. Inhibitor of Streptomyces chromofuscus phospholipase

Phospholipase D (PLD) is an enzyme that catalyzes the hydrolysis of ester bonds between phosphatidic acid and alcohols and catalyzes transphosphatidylation reactions. To gain information about the catalytic site of this enzyme, Hatanaka and co-workers investigated the effect of $[Pt(terpy)]^{2+}$ binding on the hydrolytic activity of three PLD enzymes [103]. Incubation of PLD with [Pt(terpy)Cl]Cl (curiously, the structure is presented incorrectly in the report) for 45 min results in dose-dependent and time-dependent inhibition, presumably through binding to catalytically important His residues.

4.4.4. Cysteine-modified trypanothione reductase

Trypanosomes are parasitic protozoa that cause several tropical diseases. Their metabolism involves a unique thiol reduction enzyme flavoenzyme trypanothione reductase (TR), rather than the glutathione reductase (GR) enzyme found in mammals. During catalysis, the enzyme switches between an oxidized state with a disulfide bridge between Cys-52 and Cys-57 residues and a reduced state in which bound NADPH leads to the formation of two free Cys thiols. Drugs that target unique differences between TR and GR are actively sought. Krauth-Siegel and co-workers investigated a series of ten complex cations of the type $[Pt(Yterpy)X]^{n+}$ (Y = H, Cl, 2-pyridyl, biphenyl, 4-Br-phenyl or OEt; X = NH_3, OH^-, glutathione$^-$, 4-picoline, or 2-hydroxyethanethiol; n = 1,2) for inhibition of TR from *Trypanosoma cruzi* [104]. Incubation of (reduced) TR in the presence of NADPH with a 10-fold excess of $[Pt(Clterpy)(NH_3)]^{2+}$ or $[Pt(4\text{-}Br\text{-}C_6H_4\text{-}terpy)(4\text{-}picoline)]^{2+}$ rapidly (∼10 min) and irreversibly inactivates the enzyme by 50%. Only the glutathione complex showed no cytostatic activity. Variation in the X ligand affects inhibition, with complex cations having a 2+ charge generally showing faster inhibition than do the monocations. But substituents on the terpy ligand also appear to play an important role; the authors suggest that hydrophobic groups in the 4′ position of the terpy ligand may have an affinity for the hydrophobic pocket lining the active site of the enzyme.

In the absence of NADPH, most of these complex cations cause little or no inhibition of the (oxidized) enzyme, pointing to the importance of platination of the active-site free Cys thiols in the inhibition mechanism. However, some complexes do display inhibition of the oxidized enzyme, and platination of His-460 is suggested

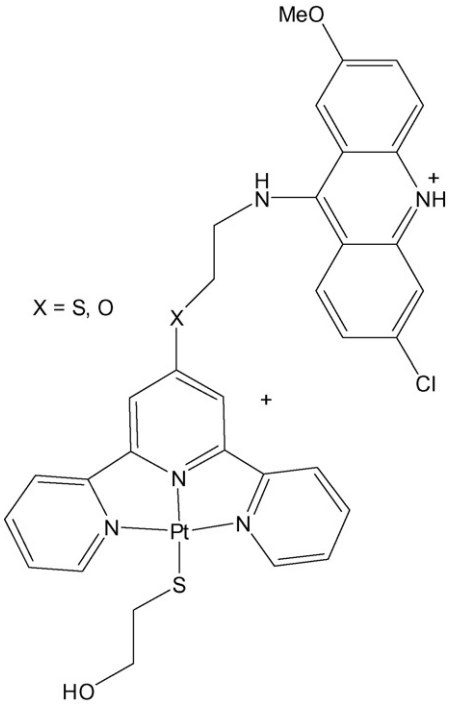

Fig. 24. Conjugate drugs having a $[Pt(terpy)(HET)]^{2+}$ unit covalently linked to an acridine trypanothione reductase inhibitor.

because coordination of disulfides by Pt(II) terpy complex cations is unprecedented. UV–vis characterization of the modified enzyme is consistent with a 1:1 binding of the Pt(II) terpy complexes to Cys-52, but not Cys-57. The platinated enzyme is stable to dialysis and treatment with thiols, but added thiols can interfere with inhibition by competing with Cys ligation of the Pt(II) terpy complex cation. The platinated enzymes also display increased oxidase activity.

Using human GR, similar studies indicate that [Pt(2-pyridyl-terpy)(4-picoline)]$^{2+}$ and [Pt(4-biphenyl-terpy)(4-picoline)]$^{2+}$ are reversible inhibitors of the reduced enzyme, while the other Pt(II) terpy complex cations show little activity [104].

A second series of Pt(II) terpyridine systems, chimeric conjugates having a covalently linked 2-methoxy-6-chloro-9-aminoacridine TR inhibitor (Fig. 24), are effective reversible inhibitors of TR and they do not inhibit human GR [105]. Interestingly, the inhibition by the conjugate drug system is different from that of the individual components in two ways. First, the irreversible inhibition of the $[Pt(Yterpy)(HET)]^+$ systems described above is lost, suggesting that the binding is no longer due to platination of the Cys-52 in the active site. Second, the reversible inhibition found for the conjugate drugs is an order of magnitude lower than other 9-aminoacridines. The authors speculate that these conjugates may accumulate in a cavity of the protein. Interestingly, variation in the nature and length of the linker connecting the $[Pt(terpy)(HET)]^+$ and 9-aminoacridine moieties affects the efficacy of inhibition.

Lowe and co-workers tested a series of 30 complexes of the type $[Pt(Yterpy)X]^{n+}$ ($n = 1$ or 2) for antiparasitic activity against three hemflagellate protozoa, but the specific binding mode was not established [66].

4.4.5. Selenoenzyme thioredoxin reductase

Human thioredoxin reductase (TrxR) is an enzyme closely related to glutathione reductase, but possesses a unique selenocysteine residue in the C-terminal sequence. TrxR reduces the protein thioredoxin, which in turn plays a role in cell proliferation. The complex involvement of thioredoxin in tumor cell growth has prompted research into the use of Pt(II) terpy complexes as inhibitors of TrxR. Becker and co-workers have synthesized the complex cations $[Pt(terpy)(4\text{-picoline})]^{2+}$, $[Pt(terpy)(HET)]^+$, $[Pt(Clterpy)(HET)]^+$, $[Pt(EtOterpy)(HET)]^+$, $[Pt(Clterpy)(S\text{-2-mercaptopyridine})]^+$, $[Pt(Clterpy)(S\text{-4-mercaptopyridine})]^+$, $[Pt(Clterpy)(S\text{-2-mercaptopyrimidine})]^+$, $[Pt(terpy)(1\text{-thiolatoglucose})]^+$, $[\{Pt(terpy)\}_2(\mu\text{-2-mercaptoimidazole})]^{3+}$, and $[\{Pt(terpy)\}_2(\mu\text{-}N,S\text{-thioacetimine})]^{3+}$ and investigated their inhibition of TrxR [106]. All of the complexes display strong and stoichiometric inhibition of TrxR in a dose-dependent manner, characterized as having both reversible competitive and irreversible tight-binding components. Because no inhibition of human GR was found, the authors hypothesized that the target for platination is the unique selenocysteine residue of TrxR. The two most potent inhibitor of the series were the $[Pt(Clterpy)(4\text{-pyridylthiol})]^+$ monocation and the dinuclear tricationic complex $[\{Pt(terpy)\}_2(\mu\text{-}N,S\text{-thioacetimine})]^{3+}$, which both inhibited proliferation of two different tumor cell lines. The research raises interesting questions as to why these two particular Pt(II) terpy complexes were more effective than other members of the family. As DNA intercalation by Pt(II) terpy complex cations is well-established (Section 2), this study identified a second cellular target for potential chemotherapeutic drugs.

A follow-up in vivo study (using a rat model) investigated the effects of two complexes of the type $[Pt(Clterpy)(SR)]^+$ (R = 4-pyridyl or 2-pyridyl) on glioblastoma cell growth [107]. These TrxR inhibitors showed marked reduction in tumor growth, but little effect on cellular glutathione concentrations. Results of this study indicate that Pt(II) terpyridine chemotherapeutic agents may have efficacy comparable to cisplatin without necessarily having severe metabolic side effects.

4.4.6. Ion channels and pumps

Sodium pump proteins are responsible for regulating ion concentration gradients in most animal cells and are driven by ATP hydrolysis. Milanick and co-workers have investigated the effect of $[Pt(terpy)Cl]^+$ on the renal sodium pump [48]. Incubation of the Na^+, K^+-ATPase enzyme with 4.5 μM $[Pt(terpy)Cl]^+$ results in nearly complete inactivation of the sodium pump in a manner consistent with a single type of reactive site. Mass spectrometry experiments on platinated pumps digested with trypsin and results from a competitive inhibition study using the platinum reagent and another cysteine-specific inhibitor allowed the researchers to conclude that platination occurs at the Cys-452 residue. The precise location of this residue is still under investigation, but the authors speculate an exterior solvent-exposed site. With $[Pt(terpy)]^{2+}$ bound, the modified pump is unable to bind ATP, and K^+ (but not Na^+, Mg^{2+}, eosin, or vanadate) increases this reaction rate. This result is dissimilar from pumps modified by iodoacetamidofluorescein, another cysteine label reagent.

ERG (*ether-à-go-go* related gene) potassium channels are involved in cardiac action potential and nerve cells. A study exploring the effect of the histidine-specific reagent diethylpyrocarbonate (DEPC) on ERG response used $[Pt(terpy)Cl]^+$ for comparison [108]. Because the two reagents displayed different effects on the peak current and deactivation rate, the author suggests that the structure of $[Pt(terpy)Cl]^+$ may results in a different type of binding than that for DEPC, but did not identify specific sites.

While several types of platinum (II) complexes, when bound to the sulfur atom of cysteine, *S*-methylcysteine or methionine in peptides promote amide bond hydrolysis under mild conditions, $[Pt(terpy)Cl]^+$ is not known to promote peptide hydrolysis [81].

4.4.7. Heavy atom scattering in X-ray crystallography

An X-ray crystal structure determination of the complex of the extra-cellular domain of human tumor necrosis factor (TNF) receptor with human TNFb used various heavy metal ions tags to enhance resolution [109]. Incubation with $Pt(terpy)Cl^+$ led to label-

ing surface histidines and resulted in a derivative that had the highest phasing power of the metal complexes investigated. This report has generated more than 675 citations since publication in 1993.

Soaking crystals of recombinant *Vibrio harveyi* acyltransferase protein in a solution of Pt(terpy)Cl^+(aq) resulted in derivatization that allowed for strong X-ray diffraction and determination of the protein structure to 3.4 Å resolution; platination occurred at four types of histidine sites [4].

5. Conclusions

During the past 30 years, Pt(II) terpy coordination compounds have become a versatile and useful family of reagents for the study of biomolecules. Research investigating their reactivity with nucleobases and amino acids is leading to an improved understanding of how these metal complexes bind to DNA and proteins and is driving progress in the design of new metallodrugs. With many new members being added to the family of Pt(II) terpy complexes in recent years, studies on their reactivity, redox properties and photophysical properties should foster their expanded use as probes of biomolecular structure and function.

References

[1] G.T. Morgan, F.H. Burstall, J. Chem. Soc. (1934) 1498.
[2] K.W. Jennette, S.J. Lippard, G.A. Vassiliades, W.R. Bauer, Proc. Natl. Acad. Sci. U.S.A. 71 (1974) 3839.
[3] S.J. Lippard, Acc. Chem. Res. 11 (1978) 211.
[4] D.M. Lawson, Acta Crystallogr., Sect. D: Biol. Cryst. 50 (1994) 332.
[5] N.M. Kostic, Comment. Inorg. Chem. 8 (1988) 137.
[6] G.R. Newkome, P.S. Wang, C.N. Moorefield, T.J. Cho, P.P. Mohapatra, S.N. Li, S.H. Hwang, O. Lukoyanova, L. Echegoyen, J.A. Palagallo, V. Iancu, S.W. Hla, Science 312 (2006) 1782.
[7] S.D. Cummings, Coord. Chem. Rev. 253 (2009) 449.
[8] E.J. Gabbay, M.A. Adkins, S. Yen, Nucleic Acids Res. 7 (1979) 1081.
[9] C.S. Peyratout, T.K. Aldridge, D.K. Crites, D.R. McMillin, Inorg. Chem. 34 (1995) 4484.
[10] L. Messori, G. Marcon, A. Innocenti, E. Gallori, M. Franchi, P. Orioli, Bioinorg. Chem. Appl. 3 (2005) 239.
[11] P.J. Bond, R. Langridge, K.W. Jennette, S.J. Lippard, Proc. Natl. Acad. Sci. U.S.A. 72 (1975) 4825.
[12] Y. Wong, S.J. Lippard, J. Chem. Soc., Chem. Commun. (1977) 824.
[13] A.H. Wang, J. Nathans, G. van der Marel, J.H. van Boom, A. Rich, Nature (London) 276 (1978) 471.
[14] A.H.J. Wang, G.J. Quigley, F.J. Koipak, A. Rich, Abstr. Am. Crystallogr. Assoc. 6 (1979) 50.
[15] J.C. Dewan, S.J. Lippard, W.R. Bauer, J. Am. Chem. Soc. 102 (1980) 858.
[16] W.D. McFadyen, L.P. Wakelin, I.A. Roos, V.A. Leopold, J. Med. Chem. 28 (1985) 1113.
[17] M. Howe-Grant, K.C. Wu, W.R. Bauer, S.J. Lippard, Biochemistry 15 (1976) 4339.
[18] M. Howe-Grant, S.J. Lippard, Biochemistry 18 (1979) 5762.
[19] W.D. McFadyen, L.P.G. Wakelin, I.A.G. Roos, B.L. Hillcoat, Biochem. J. 238 (1986) 757.
[20] W.D. McFadyen, L.P.G. Wakelin, I.A.G. Roos, B.L. Hillcoat, Biochem. J. 242 (1987) 177.
[21] L.P.G. Wakelin, W.D. McFadyen, A. Walpole, I.A.G. Roos, Biochem. J. 222 (1984) 203.
[22] A. McCoubrey, H.C. Latham, P.R. Cook, A. Rodger, G. Lowe, FEBS Lett. 380 (1996) 73.
[23] M. Cusumano, M.L. Di Pietro, A. Giannetto, Inorg. Chem. 38 (1999) 1754.
[24] H.C.M. Yau, H.L. Chan, M.S. Yang, Sens. Actuators B-Chem. 81 (2002) 283.
[25] M. Casamento, G.E. Arena, C. Lo Passo, I. Pernice, A. Romeo, L.M. Scolaro, Inorg. Chim. Acta 276 (1998) 242.
[26] M. Cusumano, M.L. Di Pietro, A. Giannetto, F. Romano, Inorg. Chem. 39 (2000) 50.
[27] J.A. Todd, L.M. Rendina, Inorg. Chem. 41 (2002) 3331.
[28] D.-L. Ma, T.Y.-T. Shum, F. Zhang, C.-M. Che, M. Yang, Chem. Commun. (2005) 4675.
[29] S.L. Woodhouse, E.J. Ziolkowski, L.M. Rendina, Dalton Trans. (2005) 2827.
[30] H. Kurosaki, N. Yamakawa, M. Sumimoto, K. Kimura, M. Goto, Bioorg. Med. Chem. Lett. 13 (2003) 825.
[31] G. Lowe, A.S. Droz, J.J. Park, G.W. Weaver, Bioorg. Chem. 27 (1999) 477.
[32] P.B. Glover, P.R. Ashton, L.J. Childs, A. Rodger, M. Kercher, R.M. Williams, L. De Cola, Z. Pikramenou, J. Am. Chem. Soc. 125 (2003) 9918.
[33] R. Stodt, S. Gencaslan, A. Frodl, C. Schmidt, W.S. Sheldrick, Inorg. Chim. Acta 355 (2003) 242.
[34] S. Gencaslan, W.S. Sheldrick, Eur. J. Inorg. Chem. (2005) 3840.
[35] J.K. Barton, S.J. Lippard, Biochem. Cell Biol. 18 (1979) 2661.
[36] J. Newman, Biopolymers 23 (1984) 1113.
[37] W.D. Wilson, B.L. Heyl, R. Reddy, L.G. Marzilli, Inorg. Chem. 21 (1982) 2527.
[38] G.W. Brady, D.B. Fein, H. Lambertson, V. Grassian, D. Foos, C.J. Benham, Proc. Natl. Acad. Sci. U.S.A. 80 (1983) 741.
[39] S. Premilat, A. Abouelkassimi, G. Albiser, C. R. Acad. Sci. Ser. III-Sci. Vie-Life Sci. 315 (1992) 265.
[40] G. Arena, L.M. Scolaro, R.F. Pasternack, R. Romeo, Inorg. Chem. 34 (1995) 2994.
[41] R. Romeo, G. Arena, L.M. Scolaro, R.F. Pasternack, Nuovo Cimento Soc. Ital. Fis. D-Condens. Matter Atomic Mol. Chem. Phys. Fluids Plasmas Biophys. 16 (1994) 1523.
[42] E.L.M. Lempers, J.S. Bashkin, N.M. Kostic, Nucleic Acids Res. 21 (1993) 1983.
[43] L.M. Scolaro, A. Romeo, A. Terracina, Chem. Commun. (1997) 1451.
[44] N. Micali, V. Villari, M. Cusumano, M.L. Di Pietro, A. Giannetto, J. Phys. Chem. B 111 (2007) 1231.
[45] C. Yu, K.H.-Y. Chan, K.M.-C. Wong, V.W.-W. Yam, Proc. Natl. Acad. Sci. U.S.A. 103 (2006) 19652.
[46] H. Bertrand, D. Monchaud, A. De Cian, R. Guillot, J.-L. Mergny, M.-P. Teulade-Fichou, Org. Biomol. Chem. 5 (2007) 2555.
[47] K.G. Strothkamp, S.J. Lippard, Proc. Natl. Acad. Sci. U.S.A. 73 (1976) 2536.
[48] N.T. Ruddock, K.L. Arnett, B.J. Wilson, M.A. Milanick, Am. J. Phys. Cell Phys. 284 (2003) C1584.
[49] G. Lowe, T. Vilaivan, J. Chem. Soc., Perkin Trans. 1 (1996) 1499.
[50] G. Lowe, J.A. McCloskey, J.S. Ni, T. Vilaivan, Bioorg. Med. Chem. 4 (1996) 1007.
[51] Z.D. Bugarcic, F.W. Heinemann, R. van Eldik, Dalton Trans. (2004) 279.
[52] D. Petrovic, B. Stojimirovic, B. Petrovic, Z.M. Bugarcic, Z.D. Bugarcic, Bioorg. Med. Chem. 15 (2007) 4203.
[53] S. Cosar, M.B.L. Janik, M. Flock, E. Freisinger, E. Farkas, B. Lippert, J. Chem. Soc., Dalton Trans. (1999) 2329.
[54] S. Wee, R.A.J. O'Hair, W.D. McFadyen, Rapid Commun. Mass Spectrom. 19 (2005) 1797.
[55] W.E. Ford, O. Harnack, A. Yasuda, J.M. Wessels, Adv. Mater. 13 (2001) 1793.
[56] D.J. Szalda, F. Eckstein, H. Sternbach, S.J. Lippard, J. Inorg. Biochem. 11 (1979) 279.
[57] S.K.C. Elmroth, S.J. Lippard, Inorg. Chem. 34 (1995) 5234.
[58] S.A. Ross, G. Lowe, D.J. Watkin, Acta Crystallogr., Sect. C: Cryst. Struct. Commun. 57 (2001) 275.
[59] P.J. Carter, C.C. Cheng, H.H. Thorp, J. Am. Chem. Soc. 120 (1998) 632.
[60] C. Le Sech, K. Takakura, C. Saint-Marc, H. Frohlich, M. Charlier, N. Usami, K. Kobayashi, Radiat. Res. 153 (2000) 454.
[61] K. Kobayashi, H. Frohlich, N. Usami, K. Takakura, C. Le Sech, Radiat. Res. 157 (2002) 32.
[62] N. Usami, Y. Furusawa, K. Kobayashi, H. Frohlich, S. Lacombe, C. Le Sech, Int. J. Radiat. Biol. 81 (2005) 515.
[63] L.R. Kelland, J. Inorg. Biochem. 77 (1999) 121.
[64] G. Lowe, A.S. Droz, T. Vilaivan, G.W. Weaver, J.J. Park, J.M. Pratt, L. Tweedale, L.R. Kelland, J. Med. Chem. 42 (1999) 3167.
[65] H. Seto, A. Tomasz, Proc. Natl. Acad. Sci. U.S.A. 74 (1977) 296.
[66] G. Lowe, A.S. Droz, T. Vilaivan, G.W. Weaver, L. Tweedale, J.M. Pratt, P. Rock, V. Yardley, S.L. Croft, J. Med. Chem. 42 (1999) 999.
[67] E.L. Crossley, D. Caiazza, L.M. Rendina, Dalton Trans. (2005) 2825.
[68] J.A. Todd, P. Turner, E.J. Ziolkowski, L.M. Rendina, Inorg. Chem. 44 (2005) 6401.
[69] A. Romerosa, P. Bergamini, V. Bertolasi, A. Canella, M. Cattabriga, R. Gavioli, S. Manas, N. Mantovani, L. Pellacani, Inorg. Chem. 43 (2004) 905.
[70] S.A. Holden, B.A. Teicher, K. Boeheim, R.R. Weichselbaum, T.J. Ervin, Br. J. Cancer 55 (1987) 245.
[71] E.M.A. Ratilla, H.M. Brothers, N.M. Kostic, J. Am. Chem. Soc. 109 (1987) 4592.
[72] S.L. Pinnow, H.M. Brothers, N.M. Kostic, Croat. Chem. Acta 64 (1991) 519.
[73] X.Y. Zhou, N.M. Kostic, Polyhedron 9 (1990) 1975.
[74] R.J. Mureinik, M. Bidani, Inorg. Nucl. Chem. Lett. 13 (1977) 625.
[75] R.A.J. O'Hair, Eur. Mass Spectrom. 3 (1997) 390.
[76] T.G. Appleton, F.J. Pesch, M. Wienken, S. Menzer, B. Lippert, Inorg. Chem. 31 (1992) 4410.
[77] J. Mueller, E. Freisinger, P. Lax, D.A. Megger, F.-A. Polonius, Inorg. Chim. Acta 360 (2007) 255.
[78] H.M. Brothers, N.M. Kostic, Inorg. Chem. 27 (1988) 1761.
[79] E.M.A. Ratilla, N.M. Kostic, J. Am. Chem. Soc. 110 (1988) 4427.
[80] E.M.A. Ratilla, B.K. Scott, M.S. Moxness, N.M. Kostic, Inorg. Chem. 29 (1990) 918.
[81] I.E. Burgeson, N.M. Kostic, Inorg. Chem. 30 (1991) 4299.
[82] N. Juranic, V. Likic, N.M. Kostic, S. Macura, Inorg. Chem. 34 (1995) 938.
[83] W. Huang, C.D. Li, J.X. Wang, L.G. Zhu, Spectrosc. Lett. 31 (1998) 1793.
[84] S.A. Ross, C.A. Carr, J.W. Briet, G. Lowe, Anti-Cancer Drug Des. 15 (2000) 431.
[85] C.C. Cheng, C.H. Pai, J. Inorg. Biochem. 71 (1998) 109.
[86] K. Tanaka, K. Shigemori, M. Shionoya, Chem. Commun. (1999) 2475.
[87] M. Shionoya, K. Tanaka, Bull. Chem. Soc. Jpn. 73 (2000) 1945.
[88] M.L. Styles, R.A.J. O'Hair, W.D. McFadyen, Eur. J. Mass Spectrom. 7 (2001) 69.
[89] N.M. Kostic, in: J.F. Riordan, B.L. Vallee (Eds.), Metallobiochemistry, Part C, vol. 226, Academic Press, San Diego, 1993.
[90] H.M. Brothers, N.M. Kostic, Biochemistry 29 (1990) 7468.
[91] K.M.C. Wong, W.S. Tang, B.W.K. Chu, N.Y. Zhu, V.W.W. Yam, Organometallics 23 (2004) 3459.

[92] M.J. Hannon, P.S. Green, D.M. Fisher, P.J. Derrick, J.L. Beck, S.J. Watt, S.F. Ralph, M.M. Sheil, P.R. Barker, N.W. Alcock, R.J. Price, K.J. Sanders, R. Pither, J. Davis, A. Rodger, Chem. Eur. J. 12 (2006) 8000.
[93] R. Haas, E.W. Adams, M.A. Rosenberry, T.L. Rosenberry, in: A. Shafferman, B. Velan (Eds.), Multidisciplinary Approaches to Cholinesterase Functions, Plenum Press, New York, 1992.
[94] M.P. Jackman, M.C. Lim, P. Osvath, D. Desilva, A.G. Sykes, Inorg. Chim. Acta-Bioinorg. Chem. 153 (1988) 205.
[95] E.M.A. Ratilla, N.M. Kostic, J. Serb. Chem. Soc. 57 (1992) 205.
[96] S.G. Sivakolundu, P.A. Mabrouk, J. Inorg. Biochem. 94 (2003) 381.
[97] A.M. Bonser, O.A. Moe, J. Chem. Educ. 73 (1996) 794.
[98] S.E. Lind, J.R. McDonagh, C.J. Smith, Blood 82 (1993) 1522.
[99] E. Almaraz, A. de Paula Queite, Q. Liu, H. Reibenspies Joseph, Y. Darensbourg Marcetta, P. Farrell Nicholas, J. Am. Chem. Soc. 130 (2008) 6272.
[100] M.L. Ghirardi, C. Preston, M. Seibert, Biochemistry 37 (1998) 13567.
[101] L. Lupinkova, J.G. Metz, B.A. Diner, I. Vass, J. Komenda, Biochim. Biophys. Acta 1554 (2002) 192.
[102] B.P. Mooney, N.R. David, J.J. Thelen, J.A. Miernyk, D.D. Randall, Biochem. Biophys. Res. Commun. 267 (2000) 500.
[103] M. Kubota-Akizawa, T. Negishi, K. Mori, T. Hatanaka, J. Enzyme Inhib. Med. Chem. 17 (2002) 329.
[104] S. Bonse, J.M. Richards, S.A. Ross, G. Lowe, R.L. Krauth-Siegel, J. Med. Chem. 43 (2000) 4812.
[105] O. Inhoff, J.M. Richards, J.W. Briet, G. Lowe, R.L. Krauth-Siegel, J. Med. Chem. 45 (2002) 4524.
[106] K. Becker, C. Herold-Mende, J.J. Park, G. Lowe, R.H. Schirmer, J. Med. Chem. 44 (2001) 2784.
[107] R. Ahmadi, S. Urig, M. Hartmann, B.M. Helmke, S. Koncarevic, B. Allenberger, C. Kienhoefer, M. Neher, H.-H. Steiner, A. Unterberg, C. Herold-Mende, K. Becker, Free Radic. Biol. Med. 40 (2006) 763.
[108] H. Meves, Neuropharmacology 41 (2001) 220.
[109] D.W. Banner, A. Darcy, W. Janes, R. Gentz, H.J. Schoenfeld, C. Broger, H. Loetscher, W. Lesslauer, Cell 73 (1993) 431.